NTNU

Norwegian University of
Science and Technology

Assay development for live IL-1B detection from individual THP-1 cells

Steven de Bakker

Biotechnology
Submission date: May 2018
Supervisor: Berit Løkensgard Strand, IBT
Co-supervisor: Kai Sandvold Beckwith, IKOM

Norwegian University of Science and Technology
Department of Biotechnology and Food Science

ABSTRACT

Protein secretion is an important process that allows for cell-cell communication and coordinated immune responses to be carried out by immune cells. Methods for the study of cytokine secretion of large cell populations have been well developed, however few methods exist to study cytokine secretion with single-cell resolution. Methods that have been developed, including mRNA assays, flow cytometry with labeled cytokines, ELISPOT assays, and microwell entrapment, have been used to study single-cell cytokine release, but each have drawbacks. One of the main drawbacks is the inability to combine cytokine detection with high resolution imagery of the secreting cells. Such a method would allow the study of intracellular structures and events in combination with cytokine secretion due to external stimuli. To address this, a system was developed that utilizes SU-8 nanopillar structures to suspend cells above a surface, enabling a modified sandwich ELISA to take place underneath individual cells. High-resolution confocal microscopy was used for cytokine detection and simultaneous cellular imaging. Although further optimization must be carried out for a fully functional system to be demonstrated, this project describes the successful development of an antibody coating for the fluorescent detection of IL-1β, and has made steps toward being able to perform live IL-1β secretion studies from THP-1 ASC GFP cells.

Table of Contents

Table of Figures

Table of Tables

INTRODUCTION

Cytokines are secreted proteins which can have various, broad effects on immune responses.[1] In order for the body to create appropriate immune responses, the synthesis and secretion of cytokines must be carefully regulated, both in time and in space. Therefore, it would be expected that cells with similar phenotypes would have similar patterns of cytokine secretion. However, immune cells have been shown to have a heterogeneous pattern of cytokine secretion at single-cell levels.[2] This heterogeneity between cells with similar phenotypes raises questions on how homeostasis in the immune system is maintained. External stimulation can be used to induce cytokine release, however the relationship between intracellular processes and cytokine secretion dynamics is poorly understood for most cytokines. This is due to the lack of systems that allow simultaneous detection of cytokine secretion and imaging of individual cells.

Measuring overall cytokine release of a large population of cells is a standard procedure that has been well characterized. However, there are few well developed experimental methods that are able detect cytokine release from individual cells, while simultaneously imaging these cells. One method that has been developed to analyze single-cell gene expression is through studying mRNA from single cells. Microfluidic devices have been designed to allow for the isolation of single cells, and the collection of mRNA from these isolated cells.[3] Such a system, however, is limited in that it does not allow for the imaging of cells. Furthermore, this procedure only measures mRNA which does not always correspond directly with protein production, due to translational and secretory control mechanisms within the cell.[4] Alternatively, flow cytometry and cytokine staining can be used to detect intracellular cytokines on a single cell level. In order to do this, intracytoplasmic staining of cytokines is performed, and flow cytometry is used to detect the presence of cytokines within the sample cell population.[5] Cytokines measured in this

way, however, may not have been produced by the cell being studied but could have been an internalized product of a different cell. Therefore, it is impossible to verify that cytokines detected in this way were synthesized by the particular cell being studied.[6]

In order to overcome the drawbacks of mRNA and flow cytometric analyses, ELISPOT was developed as a method to detect secreted cytokines from single cells. The ELISPOT method adapts the ELISA method for detecting secretory cell products in cell supernatant to allow for the localized detection of secretory cell products. In this assay, cells are grown on a surface that has been treated with capture antibody. Subsequently, the cells are stimulated, and cytokines released by the cells will be captured in close proximity to the cells. Then an enzyme conjugated detection antibody can be added, which will create a color change in the subsequently added substrate. This allows for the number of cytokine emitting cells to be quantified via image analysis.[7] A schematic of the ELISPOT procedure can be seen in figure 1. Since the cytokine is captured before diffusing far into the media, the immediate vicinity of the cell will have high concentrations of the cytokine. This allows for greater sensitivity of cytokine secretion than ELISA-based or flow-cytometry based cytokine detection methods.[8] The ELISPOT assay has also been modified to use fluorophores to allow for the detection of multiple cytokines at one time.[9] However, due to the substrate used for ELISPOT, only low-resolution microscopy is possible, making detailed study of individual secreting cells impossible.

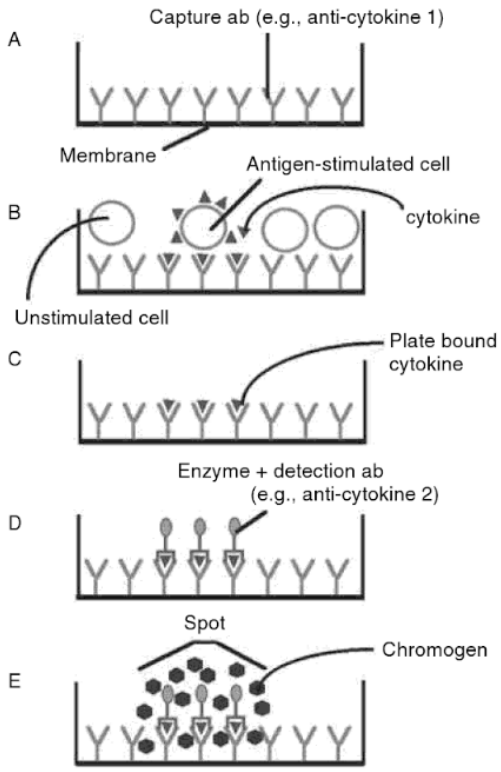

Figure 1: *A schematic of the ELISPOT assay.*[7]

Finally, entrapment of individual cells in microwells has been developed as a method to measure cytokine secretion on the single-cell level. In one study, cells were entrapped in microwells which had the bottom coated with detection antibody. A fluorescently labeled antibody was kept within the medium, which allowed for the use of TIRF microscopy to measure real-time cytokine secretion based on the strength of fluorescent signal.[10] A schematic of this method can be seen in figure 2.

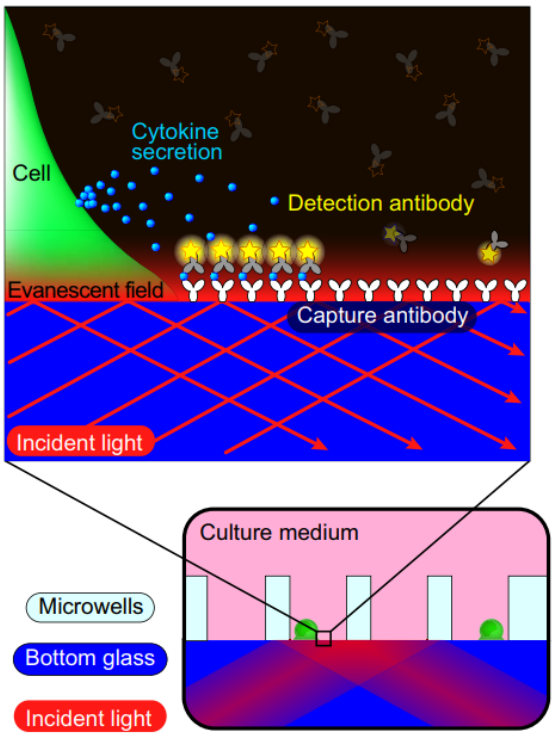

Figure 2: *A schematic of using microwells and TIRF imaging for the real-time detection of cytokine secretion.*[11]

Nanowells fabricated from PDMS have also been used for the isolation of single cells, and the study of their cytokine release. Cytokine release in these systems was measured using functionalized beads to capture secreted cytokines within the nanowells.[11]

These developed methods have been able to detect cytokine secretion from individual cells, as well as track the real-time secretion of the cytokines using micro- and nano-architectures. Few methods, however have been described that are able to simultaneously detect cytokine secretion and capture high resolution images of the secreting cells. The aim of this project is to develop such a method. To achieve this, cells will be grown and differentiated on a surface with nanopillars that have been coated to allow for the capture of specific cytokines released from the cells. Cells will be grown on nanopillars in order to create areas underneath them where cytokine detection can take place. The suspension of cells on nanopillars will result in the creation of

nanowells between the cell plasma membrane and nanopillars. In these spaces, cytokine concentration will be high, allowing for cytokine capture and subsequent detection to take place. The suspension of the cells on nanopillars will additionally be important to allow for detection medium to reach underneath the cells and allow for captured cytokines to be fluorescently labeled for detection. Unpublished observations by Kai S. Beckwith demonstrated the ability for fluorescently labeled proteins to access the space between the substrate and cells grown on 1μm high nanopillars. This system will allow for correlations between intracellular structures and cytokine secretion to be determined. The system will also more closely mimic *in vivo* conditions compared to microwell entrapment, as cells will be in close vicinity to each other, allowing for cell-cell communication to take place. A schematic of the system that will be developed can be seen in figure 3.

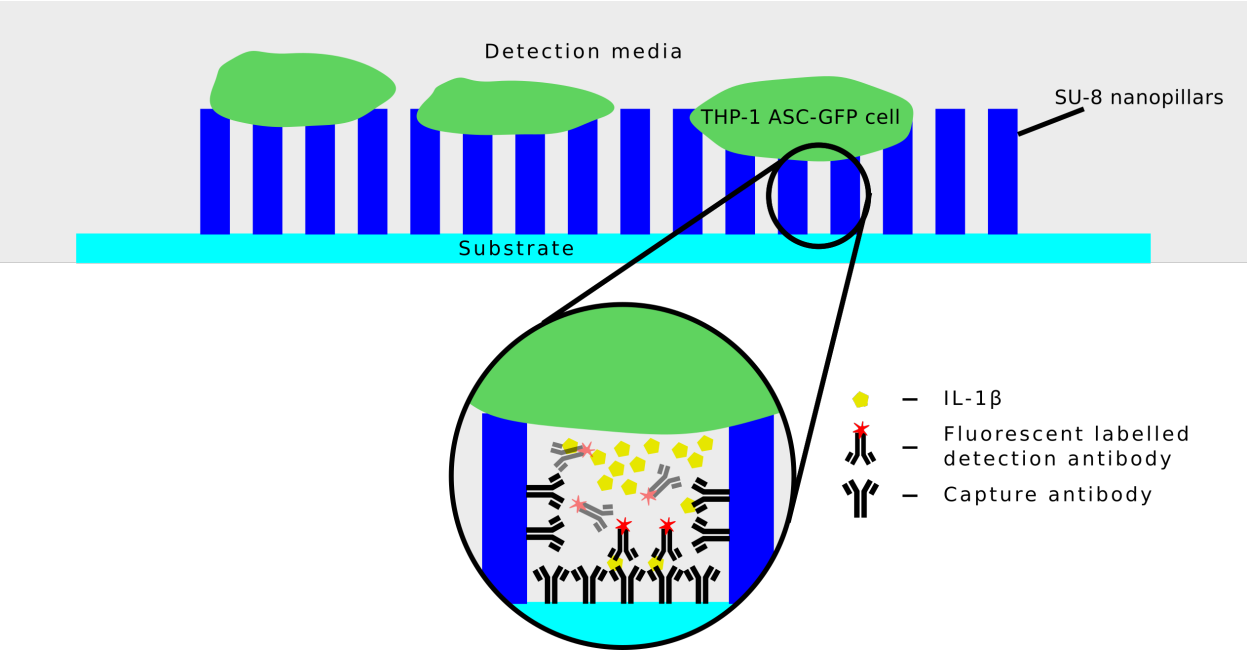

***Figure 3**: A schematic of the system that will be designed in this project.*

A standard ELISA protocol will be adapted for use on nanopillars and the cytokine secretion from individual cells will be detected through fluorescent labelling. Confocal microscopy will be

used to simultaneously image both the cells as they are releasing cytokines, and the coated surface, where released cytokines will be labeled for detection. The captured cytokines will be labeled using fluorescent streptavidin molecules.

THEORY AND BACKGROUND

Nanostructures

Nanostructures are actively being adapted for use in a wide variety of biological applications, including drug and gene delivery, the detection of proteins, probing DNA structures, tissue engineering, and studying cell interactions.[12] Due to the ability of adherent cells to interact with their surroundings, nanostructures can be used for diverse cell-based applications, such as physically probing cellular components, delivery of molecules to cells, and to modulate or measure cell adhesion on surfaces. Often nanostructures are designed to study cell behavior by creating specific topographical features on a nanoscale, allowing the cells to interact directly with the topographical features.[13] Nanostructures can be created from various materials, including inorganic and polymer materials. Materials can be selected for desired properties, such as conduction, biocompatibility, and fluorescence.[14] Electron beam lithography can be used to create nanopillars from a variety of polymers. Polymer materials offer process flexibility, and don't require high-cost dry etching equipment to be used for the creation of patterns.[15] SU-8 is one such polymer, which when combined with electron beam lithography, allows for the creation of tunable nanopillars with high stiffness, chemical durability, and optical transparency.[16, 17] As

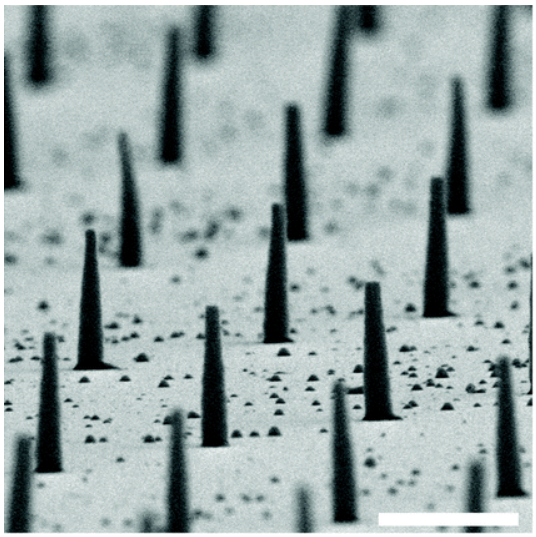

Figure 4: *SEM image of 1um high SU-8 nanopillars.* [16]

seen in figure 4, SU-8 nanopillars with high aspect ratios can be created using this method. By varying the thickness of SU-8 resist during electron beam lithography, nanopillars of different heights can be created.[17] Functionalization of SU-8 with various chemical treatments in order to increase biocompatibility, or to functionalize the SU-8 with various molecules has been shown. Oxygen plasma treatment is one such method that has been shown to increase the hydrophilicity of SU-8 as well as neural cell viability.[18, 19] Nanopatterning of surfaces allows for the control of the behavior of cells that are grown on them, and changes in the surface chemistry, flexibility, density, diameter, and height of the nanopillars can affect cell fate.[20] Portions of cells grown on 1um tall nanopillars with less than 1um spacing between the nanopillars were shown to remain suspended above the surface by the nanopillars. The suspended portion of these cells was shown to shift over time, indicating that the interaction between the cell membrane and nanopillar surface was dynamic.[16] Different membrane states could be observed, including the plasma membrane wrapping entirely around the nanopillar, the plasma membrane wrapping partially around the nanopillar, and the plasma membrane resting on top of the nanopillar without extending down its sides.[16, 21] Nanopillar density was observed to influence cell settling. When 1μm tall nanopillar spacing was increased to 2μm, cells were observed to be fully adhered to the surface.[16] Other properties, such as cell morphology, adhesion, mobility, and cytoskeletal structure have also been shown to be affected by nanopillar density.[21]

Supernatant Cytokine Detection Methods

There are many different strategies for the detection of released cytokines from populations of cells. ELISA systems are the common method used for the detection of biomolecules and offer high sensitivity, typically in the low pg/mL range. ELISA systems use a capture antibody specific to the cytokine in question to immobilize the cytokine to a surface. Then, various methods can be used to both directly or indirectly label the captured cytokines and determine the concentration of cytokine in the media. Additionally, antibody array assays, and bead-based assays offer other possibilities for cytokine detection. Antibody arrays are composed of many different immobilized antibodies, which allow for the detection of multiple different cytokines at one time. Bead-based assays offer similar possibilities, and also reduce the amount of sample needed to run the assay. The drawback of antibody array and bead-based assays, however, is that the interaction between different antibodies in close proximity to each other could lead to the detection of false positives. Due to these drawbacks, ELISA assays are often the preferred method, as long as high throughput and multiple cytokine targets are not required for the experiment.[22]

HRP ELISA system

The colorimetric ELISA system is a common method used to detect and quantify the amounts of specific proteins in solution. These systems require there to be an enzyme and substrate that creates a strong color yield for high sensitivity. Horse-radish peroxidase (HRP) is an enzyme commonly used in these assays, and 3,3',5,5'-tetreamethylbenzidine (TMB) was developed as a highly sensitive substrate for HRP in ELISA systems. The oxidation product of the TMB and HRP reaction causes a blue color to develop in the solution, based on the concentration of HRP that was present. The absorption spectrum of this product has three peaks at 370 nm, 450 nm,

and 655 nm. After the addition of a stop reagent such as H_2SO_4, however, this color changes to a bright yellow, with only one absorption peak at 450 nm.[23] By using a streptavidin-HRP conjugate and a biotin labeled detection antibody, a sandwich ELISA can be set up so that HRP is only present where detection antibody has bound to the target protein, which has been immobilized by the capture antibody. Excess, non-bound streptavidin-HRP can be washed off during the assay, causing only samples that contain the target protein to undergo a color change when the TMB substrate is added. The absorption of the color change can then be measured after a stop reagent has been added, and, when compared to the results from a standard curve, the amount of target protein in each tested sample can be determined.

Protein immobilization

To create a functional ELISA system, capture antibodies must be immobilized to the surface which is being used for the ELISA. Many different approaches can be used for protein immobilization to different surfaces, with varying advantages and disadvantages. The goal of protein immobilization is to form bonds between the protein and immobilizing surface, while maintaining protein conformation to allow for a high-performing, reproducible assay. As shown in figure 5, three main mechanisms are used for immobilization: physical, bioaffinity, and covalent immobilization.[24]

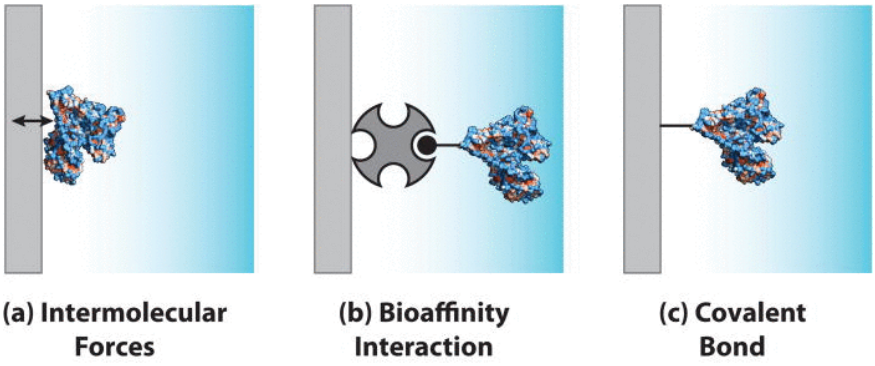

Figure 5: *A schematic of the three main mechanisms used in protein immobilization.* [25]

Physical immobilization involves the adsorption of proteins to a surface via intermolecular forces like ionic bonds, and hydrophobic and polar interactions.[24] This involves incubation of the protein with the surface to achieve attachment, eliminating the need for extra reagents to be added. The dependence of the intermolecular forces involved on environmental conditions, however, can create reproducibility issues. Random protein orientation on the surface following this method can also block active sites, or cause conformational changes in the protein, resulting in the reduction of immobilized protein activity.[26] This can be a problem, especially when designing assays to detect low concentrations of target molecules. Due to its simplicity, however, this is still the standard method used in sandwich ELISA systems.

Bioaffinity immobilization can also be used as a method to immobilize proteins onto a surface. This type of immobilization often involves the use of avidin-biotin binding. It allows for the oriented attachment of proteins, offering better interactions between the immobilized proteins and target molecules, and can also allow for immobilization reversal through chemical or physical treatments. This can allow for the creation of a reusable surface. In addition to the avidin-biotin system, protein A/G-antibody, and DNA hybridization methods have also been developed.[25]

Finally, covalent binding makes use of exposed functional groups on the side-chains of proteins to link them to the surface. This results in a strong, irreversible bond, and can provide for a high surface coverage of the immobilized protein. Multiple targeted functional groups may be present on the protein, however, causing a random orientation of the protein bound to the surface. This can reduce the activity of the protein, as active sites may not be easily accessible during the assay.[24] Unreacted functional groups can be blocked or deactivated, for example through the addition of BSA, to prevent the unreacted functional groups from binding to protein residues

during the assay.[24] but his can rely on the use of complicated or toxic reagents when preparing the immobilization surface.[27] However, the high variety of active sites that can be targeted via covalent binding makes it a common immobilization method.

3-Aminopropyltriethoxysilane (APTES) is a common chemical used for the covalent immobilization of antibodies on various surfaces.[28] The APTES system can be used in conjunction with various other chemical linkers, affinity tags, or protein absorption, making it a popular choice for immobilization chemistries.[28] Silanol groups are created on APTES by the hydrolysis of alkoxysilane groups. This silanol group can react with silanols or hydroxyls on the target surface, forming exposed amine groups, which can be used for further linkage reactions.[29, 30] This coats the oxidized surface with the APTES molecule. Subsequently, antibodies can be immobilized to the surface using various different methods, including adsorption, covalent bonding, and through the use of affinity tags. The amine group on APTES allows antibodies to be covalently bound by using bifunctional linkers such as EDC or DMP. Avidin can be used as an affinity tag, by covalently attaching it to APTES treated surface though linkers. Then, biotinylated antibodies can be bound to the surface via the strong avidin-biotin interaction.[30]

TSA Amplification

In order to be able to increase the sensitivity of immunoassays, Western blotting, and immunohistochemistry, tyramide signal amplification (TSA) was developed.[31] Signal amplification is achieved through the use of biotin-conjugated tyramide and horse-radish peroxidase (HRP). HRP reacts with hydrogen peroxide in the media and tyramide to produce tyramide radicals. These radicals are very reactive and can covalently bind to moieties that are electron rich, like tyrosine.[31] Due to the extremely short half-life of the tyramide radicals, only electron rich residues very close to the HRP will bind to the tyramide.[32] Fluorophore- or enzyme-

conjugated streptavidin can then be added in order to visualize the bound tyramide molecules. In this way, multiple fluorophore- or enzyme-conjugated streptavidin molecules can bind to a single protein of interest (and a very small area around that protein), allowing for the signal to be stronger than if the protein was labeled directly.[33, 34] The unbound TSA radicals form dimers and can be washed away.[35] For further amplification, a second round of biotin-tyramide and HRP can be added, to create an even stronger signal. A visualization of TSA amplification can be seen in figure 6.

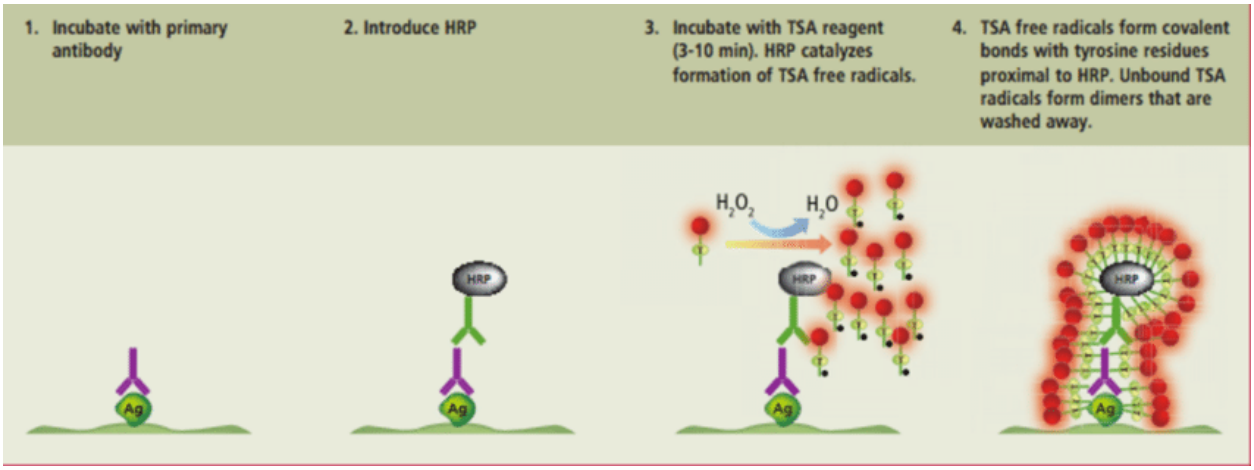

Figure 6*: A visualization of the TSA amplification process.*[35]

IL-1β

The interleukin-1 (IL-1) family of cytokines exhibit inflammatory activity once they are released into the extracellular space in numerous tissues in the body. They are produced within the cytosol, however they lack secretion signal on their N-terminal, causing a non-conventional secretory pathway to be used for their release.[36] The inflammatory functions of IL-1 in the extracellular space have been well studied, however the precise mechanism for secretion is not well known. Specifically, IL-1β is involved with antimicrobial resistance, inflammation, and Th17 cell responses. It is one of the main cytokines causing fever during inflammatory response, making it important to study.[36] IL-1β is produced by hematopoietic cells. Its precursor is not

active by itself but is activated by cleavage due to caspase-1. This leads to the release of active IL-1β into the extracellular space. Caspase-1 is activated in hematopoietic cells through cleavage of procaspase-1 by the inflammasome.[36] Therefore, the inflammasome is central to the activation and function of IL-1 cytokines like IL-1β.[37]

Following activation, IL-1 cytokines are secreted to induce inflammatory responses throughout different body tissues. Most cytokines are marked for active secretion by a secretion signal. IL-1 family cytokines, however, lack such a signal. Nonconventional secretion methods have been described for the release of IL-1 family cytokines. One such method is the cell death process of pyroptosis. In pyroptosis, caspase-1 and caspase-11 (in mice, caspase-4/5 in humans) cleave gasdermin D (GSDMD).[38] The resulting N-terminal fragment of GSDMD then forms ring-structures in the plasma membrane, which leads to plasma membrane rupture and cell lysis.[39] Cell lysis releases the cytosolic molecules of the cell into the extracellular environment, providing a mechanism for the secretion of IL-1 family cytokines. GSDMD, however, is not directly involved in the activation of IL-1β and only serves as a mechanism for its release into the extracellular space.[38] The release of IL-1 family cytokines has also been observed in viable cells, such as LPS stimulated human monocytes.[40] The mechanism for the release of IL-1 cytokines while maintaining viability is thought to involve GSDMD pores, as IL-1 cytokines have a small enough diameter to be able to pass through GSDMD pores across intact lipid bilayers.[41, 42] This mechanism has been observed when macrophages were kept under pyroptosis-inducing conditions while preventing plasma membrane rupture.[43]

Fluorescent molecules

Fluorescent molecules are commonly used in immunostaining to be able to visualize the presence of specific molecules in cells, or label specific cellular components for microscopic

analysis. Differences in chemical structures of dye molecules influence the photostability, brightness, and electrostatic interactions of the dye.[44] Fluorescent molecules work by absorbing light by moving their electrons into a higher energy state. Subsequently, the electrons fall back to their ground state, emitting light. Light absorption depends on the molecule being used, but is of a well-defined wavelength. Emitted light will be of a longer wavelength, due to some energy being lost to kinetic energy when excited electrons fall back to their ground state. The shift in the wavelength of light emitted is known as the Stokes shift.[45] Biological samples can often have their own, weak fluorescent signal, though this is generally in the blue or green region of the spectrum. This makes labeling in the red or far-red region preferred for immunostaining purposes.[46] New developments in fluorescent molecules, however, have enabled strong fluorescent signals to be able to be seen from molecules in the blue and green region as well.[45] Through the use of filters and gating, emitted light can be separated from light used in the excitation of the molecules, allowing for the visualization of the fluorescent molecule.[45] Fluorescent imaging techniques must be able to detect potentially weak signals above background noise, making fluorescent molecule selection an important step in designing an assay that will use fluorescent detection methods.[44] Multiple fluorescent molecules can be imaged at once, as long as there is sufficient separation between the emission and excitation spectra of the molecules. If this is not the case, the emission of one molecule could overlap with the emission of another molecule, causing cross-talk and making signal separation difficult.[45] For this reason, far red dyes are popular, as they are able to be combined with green or red fluorescent proteins. ATTO 647N is a type of fluorescent molecule designed for use in the far-red spectral region.[46] It is very stable, making it a good candidate for live-cell video imaging over longer periods of time.[47] Molecules labeled with ATTO 647N, however, tend to stick to glass due to the low

polarity of ATTO 647N. The molecule is also lipophilic, which can create background signals during immune staining experiments.[48]

CF640R is another fluorescent molecule designed for use in the far-red spectral region. It is significantly less hydrophobic that ATTO 647N, potentially making it a better candidate for use on glass surfaces.[44]

Confocal Microscopy

Confocal microscopy uses a pinhole to illuminate the specimen being studied, and a second pinhole to restrict the field of view that is seen. In this way, only light from the illuminated point is captured in the image, reducing light scattering from points that are not within the focal plane of the image. This allows for a reduction in blurring in the image due to light scattering, an increase in effective resolution, and the imaging of a very thin slice of specimen. Typically, the resolution in the x/y dimension is half the wavelength of light used, and the resolution in the z direction is double this. Three-dimensional images can be made by using z-stacks to capture different depths of the specimen, which can then be constructed into a three-dimensional model of the specimen using software systems. Additionally, lasers can be used to excite fluorophores within the specimen at specific excitation wavelengths. By measuring light within the emission spectra of these fluorophores, specific structures or labeled proteins within the sample can be visualized.[49] The principles of confocal microscopy, and the two pinholes limiting illuminating and detected light can be seen in figure 7. The narrow focal plane allows high resolution images to be made with little blurring due to light scattering.

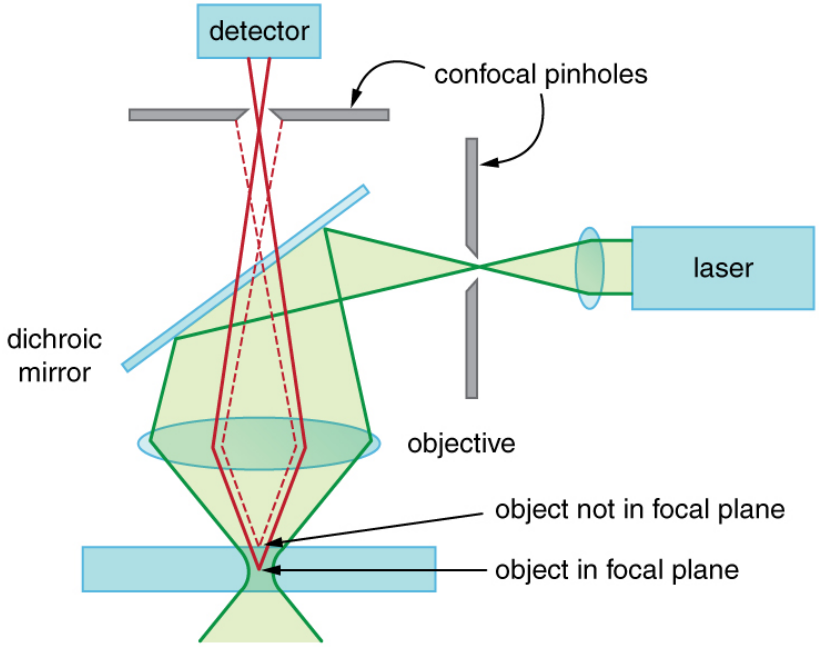

Figure 7*: A schematic of the basic optics used in confocal microscopy. Pinholes for illumination and detection allow for the imaging of thin slices of sample, which can then be reconstructed using software into a high-resolution three-dimensional image.*[50]

THP-1 Cells

Monocytes play an important role in host innate immune reactions. They help with mediating immune and inflammatory responses through the release of radicals, cytokines, and other soluble mediators.[51] For the study of monocytic cells, permanent leukemia cell lines are often used as model systems. THP-1 is a human monocytic leukemia cell line, which maintains its monocytic characteristics over long periods of time in culture.[52] This cell line can be induced to differentiate into mature macrophages through the addition of phorbol diesters.[53] Specifically, phorbol-12-myristate-13-acetate (PMA) can be used to initiate THP-1 differentiation into macrophages.[54] This occurs through the activation of protein kinase C (PKC) by PMA, leading to the activation of various signal pathways which induce the cells to differentiate into macrophages.[55] THP-1 cells incubated with PMA showed an arrest in proliferation, and became adherent and developed a macrophage morphology.[54]

MATERIALS AND METHODS

Surface Chemistry

The goal of the surface chemistry was to link the capture antibody used in a standard ELISA system to the glass or nanopillar surface. Multiple types of surface chemistries were explored for this project, to try to minimize nonspecific binding of both the detection antibody and fluorescent molecule and maximize the amount of bound capture antibody to the surface.

APTES/capture antibody

A mixture of 3-Aminopropyltriethoxysilane (APTES, Sigma-Aldrich) and capture antibody from a standard ELISA kit (DuoSet Human IL-1β, R&D systems) were used to coat the samples.[57] Initially mixtures containing both 0.5% APTES and 1% APTES (in 96% Ethanol) were tested, however 0.5% APTES was found to be adequate for antibody immobilization. In order to determine the functionality of the APTES and capture antibody mixture, the surface coating was tested on KOH cleaned glass. Initially, a test sample containing 40pg/mL of IL-1β standard was used to test the different surface coatings. A negative control without bound capture antibody was used to determine the non-specific binding properties of the KOH treated glass.

As the nanopillars would be formed out of SU-8, different cleaning methods of SU-8 and glass were compared. During typical experiments after stimulation of THP-1 cells, IL-1β supernatant concentrations around 1ng/mL were observed, so samples containing 1ng/mL of IL-1β were used as a starting point. Higher concentrations of IL-1β were expected directly underneath the cells, as the IL-1β would be secreted into a much smaller volume of media. The different types of surface treatment tested are shown in Table 1.

Table 1: *The different surfaces and treatments tested using the IL-1β TMB substrate ELISA kit.*

Surface	Treatment
glass	30 minute 1M KOH wash
glass	30 seconds oxygen plasma in a Femto plasma cleaner system at 50W
SU-8	Untreated
SU-8	30 seconds oxygen plasma in a Femto plasma cleaner system at 50W

A standard surface coating containing 0.5% APTES and 4μg/mL capture antibody was applied to each sample for a total of 30 minutes. Concurrently, a standard ELISA set-up was run in a Nunc 96-well plate, containing samples for a three-point standard curve. Samples containing 2ng/mL, 1ng/mL, and 0.5 ng/mL were added, to allow for the comparison of the binding capacity of the APTES/capture antibody coating on different surface treatments, to the standard ELISA protocol.

For the standard colorimetric ELISA, the procedure used in an industrial kit was followed (DuoSet Human IL1B kit from R&D Systems). After KOH cleaning, the samples were coated for 30 min with a mixture of APTES and capture antibody. Next, the samples were washed three times using the wash buffer (0.05% Tween in PBS). Then they were blocked using a mixture of 1% BSA (Sigma-Aldrich) in PBS for one hour. The samples were washed three times again using wash buffer, and the IL-1β samples were added to the surface. The IL-1β samples were incubated on the surfaces for two hours, after which washing was again performed three times using the wash buffer. After washing, the detection antibody was added to each surface. Incubation with the detection antibody was done for two hours. After this, the samples were washed three times using the wash buffer, and streptavidin HRP was added to the samples. They

were incubated for 20 min in the dark. Next, the samples were washed again, three times using the wash buffer, and the TMB substrate (Thermo-Fisher) was added to each sample. After a 20 min incubation with the TMB substrate in the dark, stop solution was added to each samples and the absorbance was measured using a UV/vis plate reader. The absorbance was measured at 470nm, with a correction at 540nm.

In order to visualize the secretion of IL-1β from live cells, a colorimetric detection molecule could not be used, as this would not allow for localization of the signal. Therefore, a fluorescent streptavidin conjugate was used. Initially, ATTO 647N streptavidin (Sigma-Aldrich) was used for this purpose. Using the standard APTES/capture antibody coating on KOH treated glass, different concentrations of ATTO 647N streptavidin were added during the detection step, in order to determine the optimal concentration for use in the later live cell assays. Concentrations of 12μg/mL, 6μg/mL, 3μg/mL, 1.5μg/mL, and 0.75μg/mL were tested. After incubation with the fluorescent streptavidin for 30 minutes, samples were imaged using a confocal microscope. The surface of the glass was brought into focus, and the fluorescence of the bound streptavidin to the surface was visualized. Negative controls were also included in the experiment. One negative control was KOH-treated glass without the APTES/capture antibody coating, while the second negative control had the APTES/capture antibody coating but did not have any IL-1β standard added to it. In this way, any nonspecific binding between the KOH treated glass surface and ATTO 647N streptavidin and between the APTES/capture antibody coating and ATTO 647N streptavidin could be visualized.

DMP

In order to increase binding of capture antibody to the surface, as well as decrease nonspecific binding, a second type of surface coating using dimethyl-pimelimidate (DMP, Sigma-Aldrich) was tested. For this coating method, the glass was first cleaned with KOH, then coated with 2% APTES in 96% Ethanol for two hours. This coating was left to cure overnight at 37°C. After, a mixture of 100μg/mL DMP and 4μg/mL capture antibody was used to coat the wells. A standard curve was run using concentrations of 2ng/mL, 1ng/mL, 500pg/mL, 250 pg/mL, 125 pg/mL, 62.5pg/mL, and 31.25pg/mL of IL-1β standard. Additionally, two negative controls were used to determine the nonspecific binding of detection antibody to the surface. For the first negative control, the standard protocol was used, with a sample of 1ng/mL IL-1β standard, but without surface coating with the DMP/capture antibody mixture. For the second negative control, the DMP/capture antibody coating was applied, however no IL-1β standard was added.

Nanopillar Sample Mounting

The nanopillars used during this experiment were 1um and 2um tall, with 1um spacing between the pillars, in a hexagonal pattern. The pillars were made out of SU-8 on glass coverslips. Squares of 1mmx1mm nanopillar grids were used during this project. The nanopillars used in this project were created by Jakob Vinje, at the NTNU Biophysics department. In order to culture cells on the nanopillars and test them for functionality in the developed ELISA protocol, it was necessary to mount the samples in 96-cell plates. Standard polystyrene 96-well plates were used, and the bottom was removed using a drill. Liquid paraffin was applied to the periphery of the hole created, and the glass with nanopillar grid was mounted to the 96-well plate in this way. Before use in experiments, mounted samples were sterilized with 70% ethanol and rinsed with sterile PBS.

Conjugate of SA CF640R and detection antibody

As another method to reduce nonspecific binding in the assay, and to allow for simple live cell imaging, a conjugate of the detection antibody and fluorescently labeled streptavidin was made. This was done by incubating the detection antibody with an excess of fluorescently labeled streptavidin for a duration of three hours, in the dark. After this, 100kda filters (Sigma-Aldrich, Amicon Ultra 0.5mL centrifugal filters) were used to remove unbound fluorescent streptavidin and collect the conjugate. After the three-hour reaction time, 500μL of the solution was loaded into each 100kda filter, and spun at 14000*g for 10 minutes. Afterwards, filters were removed and inverted into empty Eppendorf tubes and spun at 1000*g for 1 minute to remove the detection antibody/CF640R conjugate. The conjugate was diluted back to the initial starting concentration of 300ng/mL detection antibody and stored in the dark at -20°C. The concentrations used are listed in Table 2.

***Table 2**: The components and concentrations of the reaction solution used to create the detection antibody-streptavidin CF640R conjugate.*

Reagent	Concentration
Detection Antibody	600ng/mL in 1% BSA
Streptavidin CF640R	18μg/mL in 1% BSA

This created a final reaction solution of 300ng/mL detection antibody and 9μg/mL of Streptavidin CF640R in 1% BSA.

TSA Amplification

In order to amplify the fluorescent signal from bound streptavidin molecules, TSA amplification was used. The standard fluorescent ELISA procedure was followed until the addition of the fluorescent streptavidin molecule. Instead, streptavidin HRP was added for 20 min while the samples were kept in the dark. Then, the samples were washed three times with 300μL wash buffer. Next, the samples were washed twice using 300μL TSA wash buffer. Then, samples were incubated with 100μL TSA working solution for 30 min in the dark. After this, the samples were washed three times with 300μL wash buffer, and then incubated with 100μL of the Streptavidin CF640R solution for 30 min. Finally, the samples were washed three times with 300μL wash buffer and then stored in PBS for imaging. The concentrations of solutions used are listed in Table 3.

Table 3*: Compositions of solutions used in the TSA amplification procedure. All solutions were made immediately before use.*

Solution	**Composition**
Wash Buffer	0.05% Tween in PBS
TSA Wash Buffer	0.1% Tween + 100mM borate (pH 8.5) in distilled water
Streptravidin-HRP	1:40 dilution in 1% BSA
TSA Working Solution	0.1% Tween + 0.003% H_2O_2 + 0.5mM biotin tyramide in 100mM borate (pH 8.5)
Streptavidin CF640R	12μg/mL in 1% BSA

Cell Work

Cell Culture

THP-1 ASC-GFP cells were maintained in suspension culture for the duration of this project. The cells were maintained in RPMI, supplemented with 10% FCS and 1% pen/strep. The cells were passaged every 3-4 days, to maintain a cell concentration between $2x10^5$ cells/mL and $1x10^6$ cells/mL.[57]

For growth on glass surfaces and nanopillars, THP-1 ASC-GFP cells were differentiated into macrophages. This was done through stimulation with PMA. Cells were mixed with 100 ng/mL PMA and seeded onto the surface at a concentration of $3.5x10^5$ cells/mL. After 72 hours, the cell media was refreshed with new RPMI (with 10% FCS and 1% pen/strep) and the cells were allowed to rest overnight. The following day the cells were stimulated to release IL-1β and imaging was performed using confocal microscopy.

Cell Stimulation

After differentiation into macrophages, cells were stimulated to release IL-1β. This was done by adding E.coli K12 LPS (Invivogen) and nigericin (Sigma-Aldrich) to the cells.[40] First, cells were incubated with 1μg/mL LPS for a duration of 3 hours. After that, they were incubated with 10 uM nigericin for 1 hour. This stimulated them to release IL-1β, which could then be measured by removing the supernatant and running a HRP/TMB ELISA, or captured on a surface and labeled fluorescently for imaging using confocal microscopy.

Cell Fixation

To be able to both visualize the cells and fluorescently label the IL-1β bound to the capture antibody, the cells were fixed. This was done using PFA. After stimulation with LPS and nigericin, the supernatant was withdrawn, and cells were rinsed using sterile PBS. Then, a 4%

PFA in PBS mixture was added to the cells for 15 min to fix them. This was then drawn off, and the fixed cells were again rinsed using sterile PBS.

PFA quenching

PFA quenching was used to reduce the binding of the detection antibody and fluorescent streptavidin conjugate to the PFA. This was done with a quenching medium, made up of 100mM glycine and 100mM NH_4Cl in PBS. This mixture was added after the PFA fixation had taken place and incubated for 10 minutes. Afterwards the cells were washed with sterile PBS, and the standard steps for adding the detection antibody followed by the fluorescent streptavidin were followed.

Live Signaling Detection

To attempt to detect the signals from the fluorescent streptavidin molecules during live cell imaging, a live signaling detection media was made. This was done by re-suspending the fluorescent streptavidin-detection antibody conjugate in Hanks Balanced Salt Solution (Sigma-Aldrich). After stimulating the cells with LPS, the media was replaced with 100μL of fluorescent streptavidin-detection antibody conjugate in Hanks Balanced Salt Solution (150ng/mL SA-detection antibody conjugate), 10uM of nigericin stock was added to each well to complete cell stimulation, and imaging of the cells was begun on the confocal microscope. The microscope was heated to 37°C, and a 5% CO_2 environment was maintained for the duration of the imaging.

Confocal Microscopy

After the cells were stimulated with LPS and nigericin, confocal microscopy was used to detect the fluorescent signal emitted by the streptavidin bound to detection antibodies.

To find the correct focal plane, the reflection signal from the surface was found, and imagine was performed from this height to 2-3um higher, to account for the 2um tall nanopillars. In this region the fluorescent signal should have been visible.

For live cell imaging, a time-lapse of various tiles was used. A z-stack was set up to image the area from the glass surface, to 3um above to capture the full nanopillars, and parts of the cells growing on the nanopillars. The time-lapse was started just after nigericin addition, so that cells could be monitored for ASC speck formation using the GFP fluorescence. Simultaneously, the nanopillars were imaged to try to detect the binding of IL-1β and the detection antibody/CF640R streptavidin conjugate. In order to give sufficient time for IL-1β release from the cells, and the binding of IL-1β to the capture antibody and subsequent binding of the detection antibody/CF640R streptavidin conjugate to the bound IL-1β, time lapses were run for a total of 3 hours. The microscope's autofocus feature was set to the center of the z-stack to try to maintain focus at that point.

In addition to live imaging, cells were also imaged following the PFA fixation and PFA quenching protocols.

RESULTS

Glass surface ELISA

Comparing glass to standard ELISA

Although a two-step method is more common for APTES-based antibody immobilization, a simple, single step method has recently been published with promising results.[57] This method is based on premixing APTES and the antibody, and was tested as a simple starting point for IL-1β capture antibody immobilization. To test initial functionality of the APTES/capture antibody mixture, an ELISA was run using mixtures containing 0.5% APTES and 1% APTES, and a negative control which was not treated with any capture antibody. A standard sample containing 62.5 pg/mL IL-1β was added to each surface coating during the ELISA procedure. The results of the measured concentration of IL-1β standard of each sample, when compared to a standard curve performed on a standard Nunc 96-well plate are shown in Table 4.

Table 4: *The calculated concentration of IL-1β on each surface coating, after performing a TMB based ELISA using a standard sample of 62.5pg/mL IL-1β.*

Surface Coating	Average Absorption at 450nm	Concentration IL-1β	Standard Deviation (concentration)
1% APTES + 4μg/mL capture antibody	0.322	44.75 pg/mL	16 pg/mL
0.5% APTES + 4μg/mL capture antibody	0.372	38 pg/mL	2 pg/mL
No coating (control)	0.367	44.25 pg/mL	

The measured calculated concentration of IL-1β in each sample was approximately the same for each sample. This indicated that the nonspecific binding of IL-1β standard to the KOH, 1% APTES, and 0.5% APTES treated glass was approximately 40pg/mL. Since the coated samples

and negative control captured the same amount of IL-1β, it was determined that the tested sample of 62.5pg/mL IL-1β was below the sensitivity of this assay. For this reason, farther testing was done using 1ng/mL of IL-1β, which, as discussed later, was closer to the expected concentration of IL-1β underneath secreting cells. Since the nonspecific binding of IL-1β was the same for both 0.5% APTES and 1% APTES surface treatments, further coatings were made using only 0.5% APTES mixed with capture antibody. The higher concentration of 1ng/mL IL-1β was added to glass coated with 0.5% APTES mixed with capture antibody to demonstrate the ability of this coating method to detect a higher concentration of IL-1β. The results of this can be seen in table 5.

Table 5: *The absorption results for KOH cleaned glass treated with 0.5% APTES + capture antibody, after performing a TMB based ELISA using a standard sample of 1ng/mL IL-1β.*

Surface Coating	Average absorption at 450 nm	Standard Deviation
0.5% APTES + 4μg/mL capture antibody	1.948	0.091

DMP Surface coating

The antibody immobilization method using the bifunctional crosslinker DMP was also tested on glass surfaces as an alternative to the APTES method for covalent immobilization of the capture antibody. A standard curve using IL-1β standard was performed, as well as a negative control to determine the nonspecific binding of IL-1β to antibodies immobilized to this surface. Results of this experiment can be seen in Table 6.

Table 6: *The average absorption, measured at 450 nm, of concentrations of IL-1β ranging from 2ng/mL to 0ng/mL for glass samples prepared using the DMP surface coating method.*

Concentration of IL-1β standard added during ELISA	**Average absorption measurement at 450 nm**	**Standard Deviation**
2 ng/mL	2.054	0.005
1 ng/mL	1.451	0.093
0.5 ng/mL	1.030	0.037
0.25 ng/mL	0.564	0.048
0.125 ng/mL	0.278	0.014
0.0625 ng/mL	0.156	0.004
0.0313 ng/mL	0.082	0.005
0.0 ng/mL (negative control)	0.023	0.003

The DMP coating functioned to immobilize the capture antibody onto the glass surface, and had a low standard deviation for each point, indicating high assay stability. Additionally, the absorption when no IL-1β was added during the ELISA was lower than the lowest point on the standard curve, indicating the nonspecific binding of IL-1β to glass treated in this method was very low. The added complexity of this coating method, however, made it a second choice to the 0.5% APTES/capture antibody coating, as the coating using APTES was a one-step method requiring only a short incubation time.

SU-8 and nanopillar ELISAs

Comparison of different surface treatments of SU-8

To test the functionality of different surface treatments of glass and flat SU-8 on the standard ELISA assay, a standard HRP ELISA was run on each surface, with a mixture of 0.5% APTES and 4μg/mL capture antibody used to coat the surface at the start of the ELISA. Negative controls for each type of treatment were still coated with APTES and capture antibody, however no IL-1β standard was added to determine nonspecific binding of the detection antibody and streptavidin-HRP to the surface treatment. The absorbance was measured for each type of surface treatment, as listed in Table 7.

Table 7: *The absorbance of various surfaces and surface treatments, after running a standard HRP ELISA using 1ng/mL IL-1β concentration. Negative controls where no IL-1β was added during the assay are also included.*

Surface Coating	IL-1β (+/-)	Average absorbance at 450 nm	Standard Deviation
KOH glass	+	1.948	0.091
negative control KOH glass	-	0.121	0.059
Plasma cleaned glass	+	0.971	0.543
Negative control plasma cleaned glass	-	0.034	0.001
Untreated SU-8	+	0.715	0.636
Negative control untreated SU-8	-	0.043	0.002
Plasma cleaned SU-8	+	1.061	0.173
Negative control plasma cleaned SU-8	-	0.031	0.014

KOH treated glass had the highest absorbance at 450 nm, followed by plasma cleaned SU-8, plasma cleaned glass, and untreated SU-8. The standard deviations for plasma cleaned glass and

untreated SU-8 were quite high, at 0.543 and 0.636 respectively. The high standard deviation for SU-8 was likely due to the presence contaminants on the SU-8 surface from lack of cleaning interfering with the assay. It is unclear what caused the high standard deviation of plasma cleaned glass, as a similar result was not seen in plasma cleaned SU-8. It is possible that an even treatment was not achieved on the glass samples tested. The negative controls for each surface treatment were significantly below the mean absorbance of the normal surface coating. This indicated that the nonspecific binding of both detection antibody and streptavidin-HRP to the differently treated surfaces was very low. The best performing surface treatment for glass was 1M KOH, while the best performing surface treatment for SU-8 was plasma cleaning. The KOH treatment was not tested for SU-8, as it could lead to detachment of SU-8 from the substrate.

Imaging of fluorescent detection system

Prior to attempting to image live cells secreting IL-1β, the fluorescent system was tested on glass and nanopillars. The standard fluorescent ELISA procedure was followed. Initially ATTO 647N streptavidin conjugate was used to determine the correct concentration of fluorescent molecule to use in the assay. Results of this imaging on 1M KOH cleaned glass can be seen in figure 8.

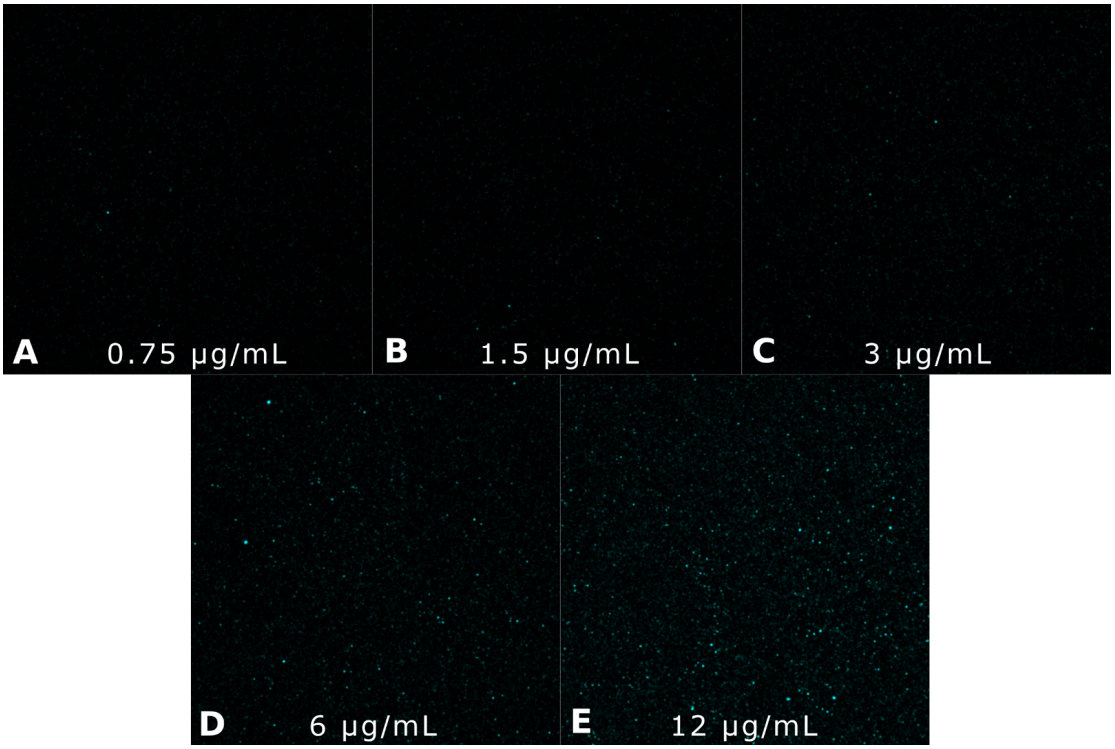

***Figure 8**: The fluorescent signal on a glass surface of different concentrations of ATTO 647N tested using 1ng/mL IL-1β. A-E show ATTO 647N concentrations of 0.75µg/mL-12µg/mL.*

A slight increase in fluorescent signal can be seen when increasing the concentration of ATTO 647N used in the assay up to 12µg/mL. A weak fluorescent signal can be seen in figure 8E, where 12µg/mL of ATTO 647N was added during the assay.

Due to this weak visible signal, further testing of the fluorescent system was done using a concentration of 12µg/mL of ATTO 647N. A series of concentrations of IL-1β ranging from 0.25ng/mL IL-1β standard to 8ng/mL of IL-1β standard were tested on KOH treated glass to determine the sensitivity of the assay. The results of this can be seen in figure 9.

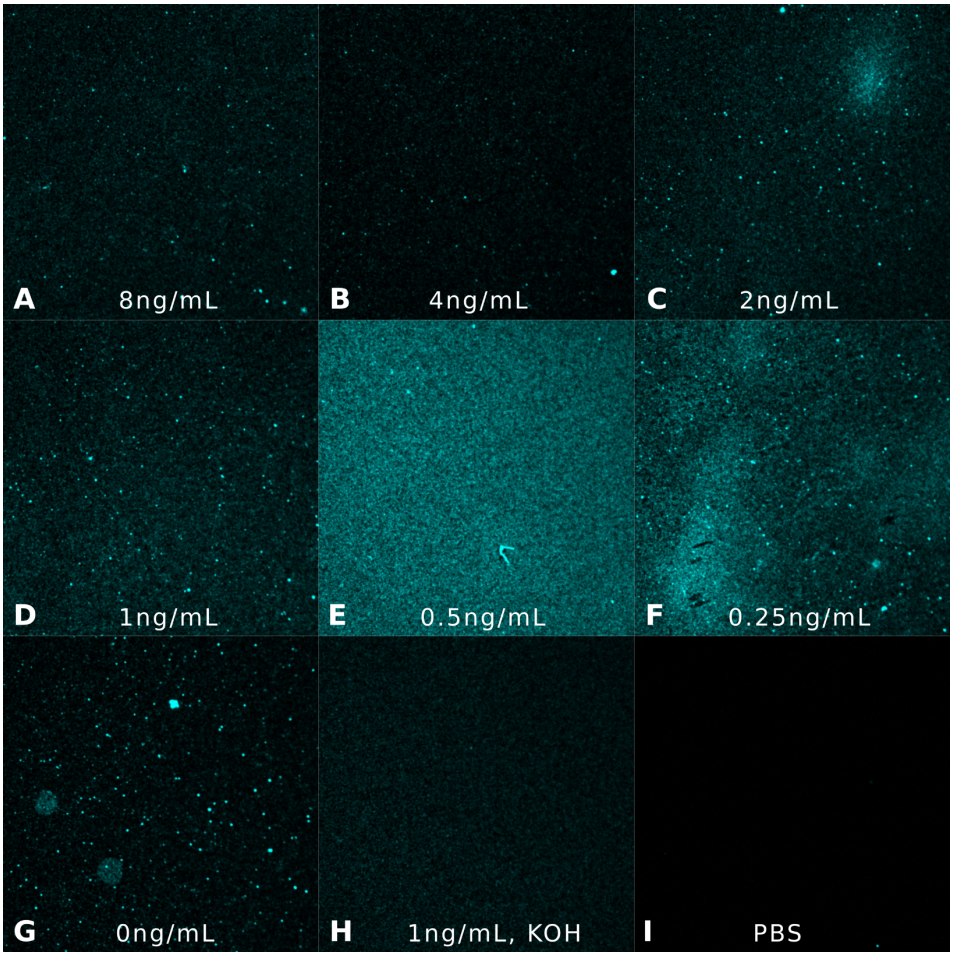

***Figure 9**: Fluorescent signals from a series of IL-1β concentrations tested using 12µg/mL of ATTO 647N. IL-1β concentrations from 8ng/mL to 0.25ng/mL (A-F) were tested. G) shows a negative control, where no IL-1β standard was added. H) shows a second negative control, where no APTES/capture antibody was used to coat the surface, but 1ng/mL IL-1β standard was added to the sample. I) shows a blank of a well containing just PBS.*

Fluorescent signals can be seen for all concentrations of IL-1β tested in this assay, including the negative control where no IL-1β was added. No decrease in fluorescent signal can be seen when the concentration of IL-1β added during the assay was decreased. This indicates there was significant nonspecific binding between the ATTO 647N streptavidin molecule and the APTES/capture antibody treated surface used during this assay.

Due to the nonspecific binding of ATTO 647N streptavidin to the APTES/capture antibody surface coating, a less hydrophobic molecule, CF640R streptavidin, was used for further testing.

First, a positive signal was confirmed by imaging CF640R streptavidin that had been dried on a glass surface. The results of this imaging can be seen in figure 10.

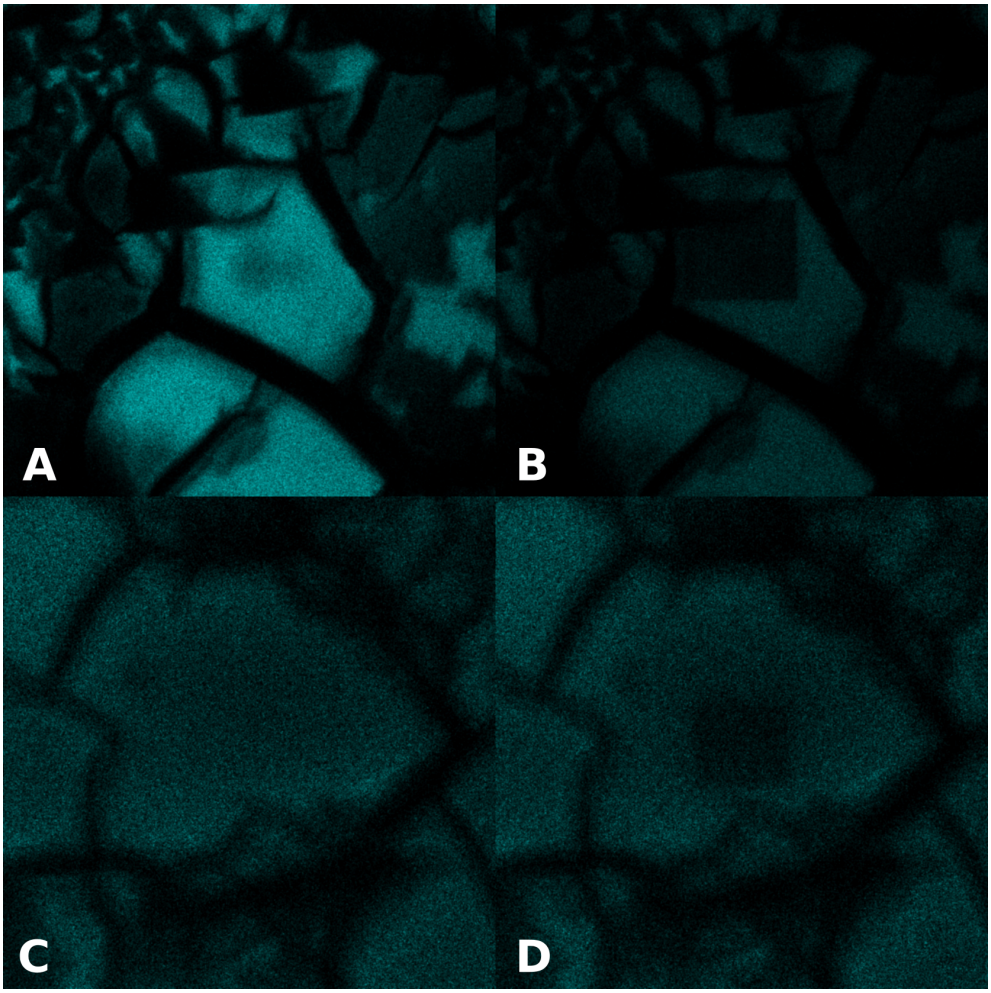

***Figure 10**: Fluorescent imaging of dried CF640R streptavidin. Crystalline structures and fluorescent signals can be seen in the images. A) Shows a concentration of 12µg/mL of CF640R dried onto a piece of glass. B) Shows the same sample, however a square area in the middle was bleached using high laser power in order to confirm a fluorescent signal. C) Shows the dried CF640R streptavidin/detection antibody sample. D) Shows the same sample, with a square in the middle that has been bleached to confirm a fluorescent signal.*

In figures 10B and 10D, a dark square can be seen in the middle of the image. This was created by bleaching the fluorophore, by zooming in on that section and exposing the sample to a high laser power. This was done to ensure that the signal seen in figures 10A and 10C were due to

fluorescence, and not due to reflection of the laser off of the glass surface, or the crystalline structure formed by the dried fluorescent molecules.

After confirming that a fluorescent signal could be seen using confocal microscopy, further testing was done using the CF640R streptavidin molecule in the ELISA system. The system was tested to determine whether 1ng/mL IL1B standard could be detected on KOH cleaned glass coated with APTES/capture antibody, and negative controls were also tested to determine if any nonspecific binding was present. The results of this can be seen in figure 11.

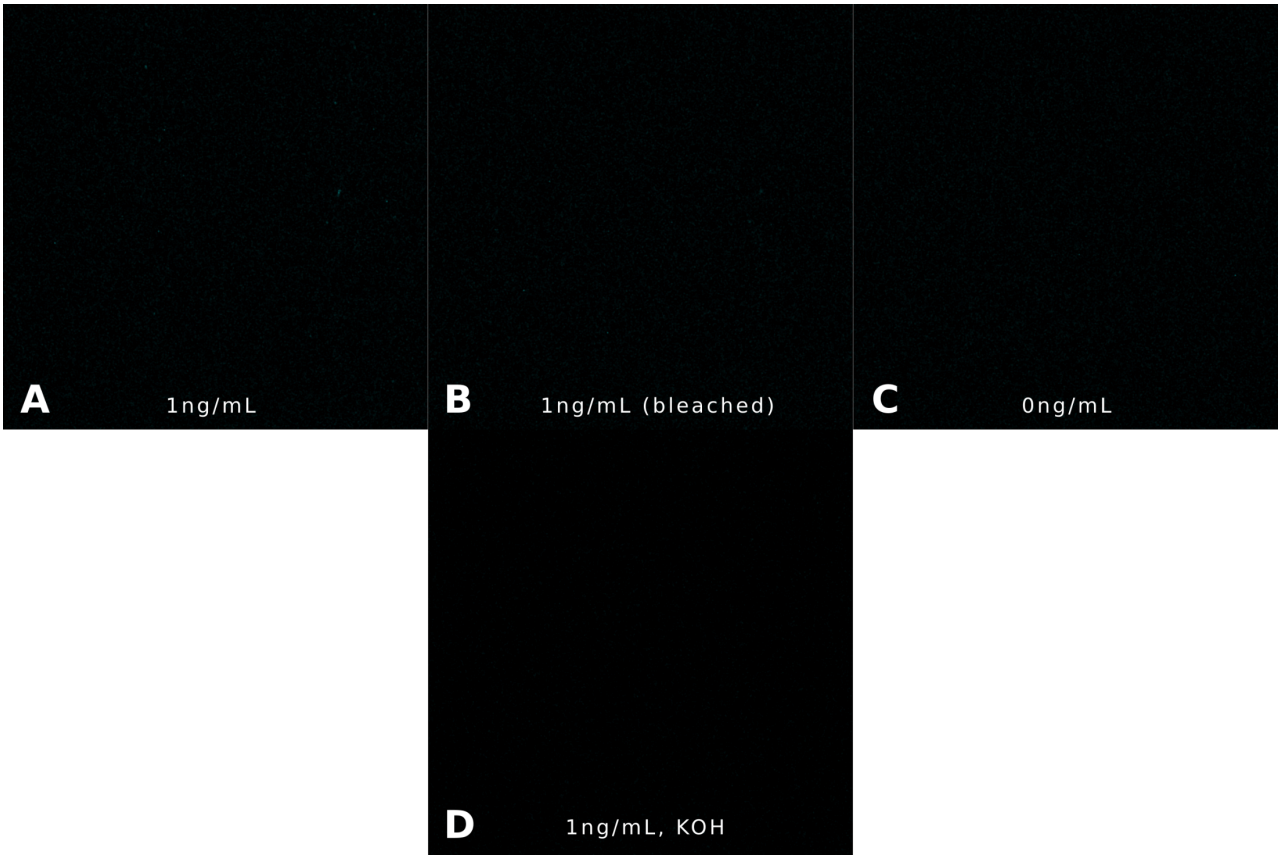

Figure 11: *Fluorescent signal of CF640R tested with 1ng/mL of IL-1β and negative controls. A) shows the weak signal from an ELISA run with 1ng/mL of IL-1β standard and 12μg/mL CF640R streptavidin. B) Shows an attempt at bleaching the signal from A. C) Shows a negative control where no IL-1β standard was added. D) shows a second negative control where 1ng/mL IL-1β standard was added, but the surface had not been coated by APTES/capture antibody.*

A weak fluorescent signal is visible in figure 11A, where 1ng/mL IL-1β had been added. Again, a section of the sample was bleached to determine if the signal seen was fluorescent. No clear

bleaching was seen in figure 11B, indicating that the weak signal visible in 11A was likely due to either noise, or a weak reflection of laser light off of the glass surface. No visible signal can be seen in figure 11C, indicating that there was no significant nonspecific binding between CF640R streptavidin and the APTES/antibody treated surface. No signal was seen in figure 11D, indicating that there was no nonspecific binding between CF640R streptavidin and the KOH treated glass surface.

When comparing the nonspecific binding of CF640R and ATTO 647N bound streptavidin molecules, it was clear that CF640R had much lower nonspecific binding, as can be seen in figure 12.

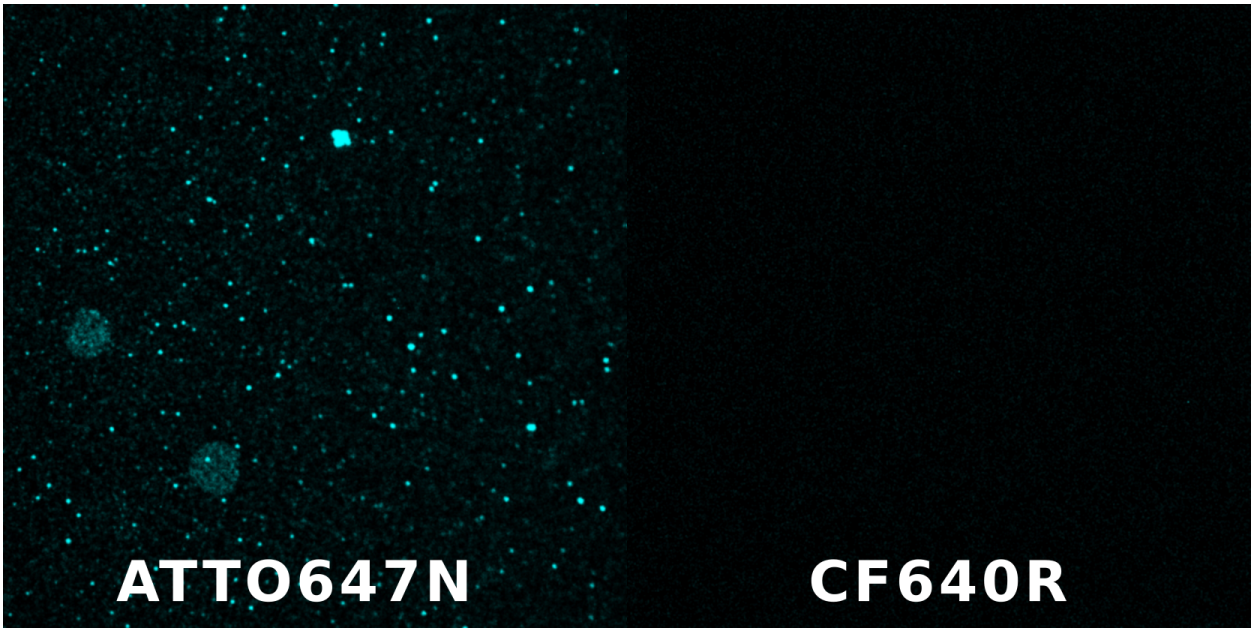

Figure 12: *A comparison of the fluorescent signals due to nonspecific binding between APTES/capture antibody coated glass when adding ATTO647N vs. CF640R to APTES/capture antibody coated KOH cleaned glass.*

Due to the weak signals seen when running an ELISA using 1ng/mL IL-1β standard and 12μg/mL CF640R streptavidin, TSA amplification was used to amplify the weak signal from this system. The result of TSA amplification can be seen in figure 13.

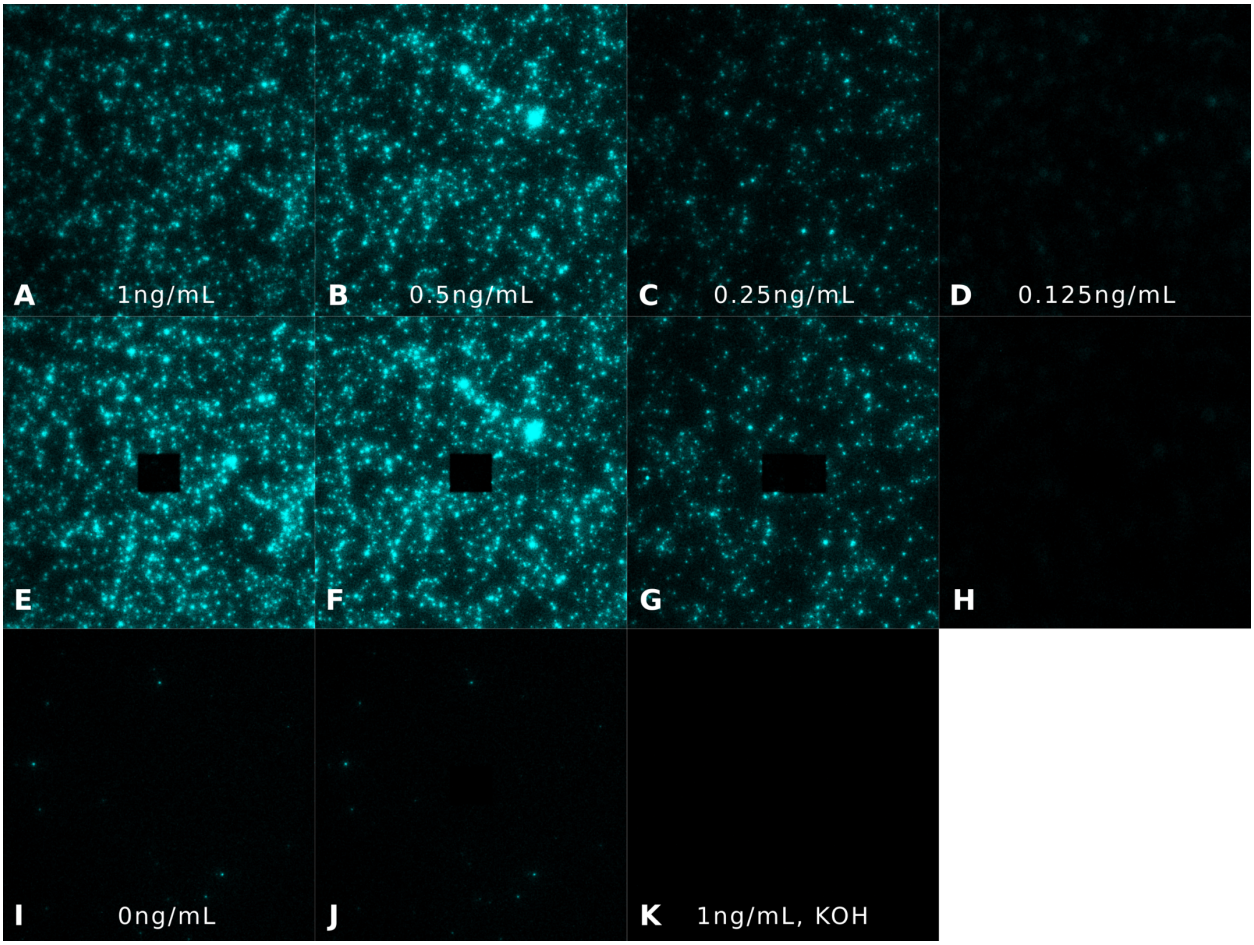

Figure 13*: Fluorescent signal after TSA amplification of different concentrations of IL-1β. A) shows the fluorescent signal from CF640R after TSA amplification when 1ng/mL IL-1β was added during the ELISA. B) shows the fluorescent signal when 0.5ng/mL IL-1β was added. C) shows the fluorescent signal when 0.25ng/mL IL-1β was added. D) shows the fluorescent signal when 0.125 ng/mL IL-1β was added. E) shows A after bleaching a central square. F) shows B after bleaching a central square. G) shows C after bleaching a central square. H) shows D after bleaching a central square. I) shows the fluorescent signal when no IL-1β was added. J) shows I after bleaching a central square. K) shows the fluorescent signal when 1ng/mL IL-1β was added but the surface was not coated with APTES/capture antibody.*

A decrease in fluorescent signal can be seen between figures 13A-D, corresponding to the decreasing amount of IL-1β being added to the samples. The lack of difference between figures 13A and 13B could have been due to saturation of the TSA system, making it impossible to bind more fluorescent molecules at concentrations above 0.5ng/mL of bound IL-1β. The ability to see a difference in fluorescent signal between figures 13B and 13C indicates that this method has a high enough resolution to detect differences of 0.25ng/mL IL-1β. The weak signal seen in figure

13D indicates that the limit of IL-1β detection using this method was around 0.125ng/mL. Bleaching was again used for each sample in order to confirm that the observed signal was due to fluorescence, and not reflection off of the glass surface.

Next, TSA amplification was performed on 2um tall, plasma cleaned SU-8 nanopillars which had been coated with APTES/capture antibody. To simulate live cell imaging experiments, a higher concentration of 100ng/mL IL-1β standard was used. This higher IL-1β concentration was used due to measured concentrations of IL-1β found in the supernatant after LPS and nigericin stimulation. As reported later, the concentration of IL-1β found in the supernatant of LPS+nigericin stimulated cells was about 4ng/mL. By assuming the THP-1 cells form a 10μm high monolayer, and medium fills the wells of a 96 well plate to 3 mm, the ratio of cell volume to well volume is about 300. Thus, by multiplying this ratio with 4ng/mL IL-1β, it was estimated 1.2μg/mL would be concentrated within the cells. If only 30% of cells were stimulated, this would reduce the intracellular concentration to 360ng/mL. Since capture would take place about 2μm from the cell surface, a conservative concentration of 100ng/mL was used to simulate live cell imaging conditions. The results of this assay can be seen in figure 14.

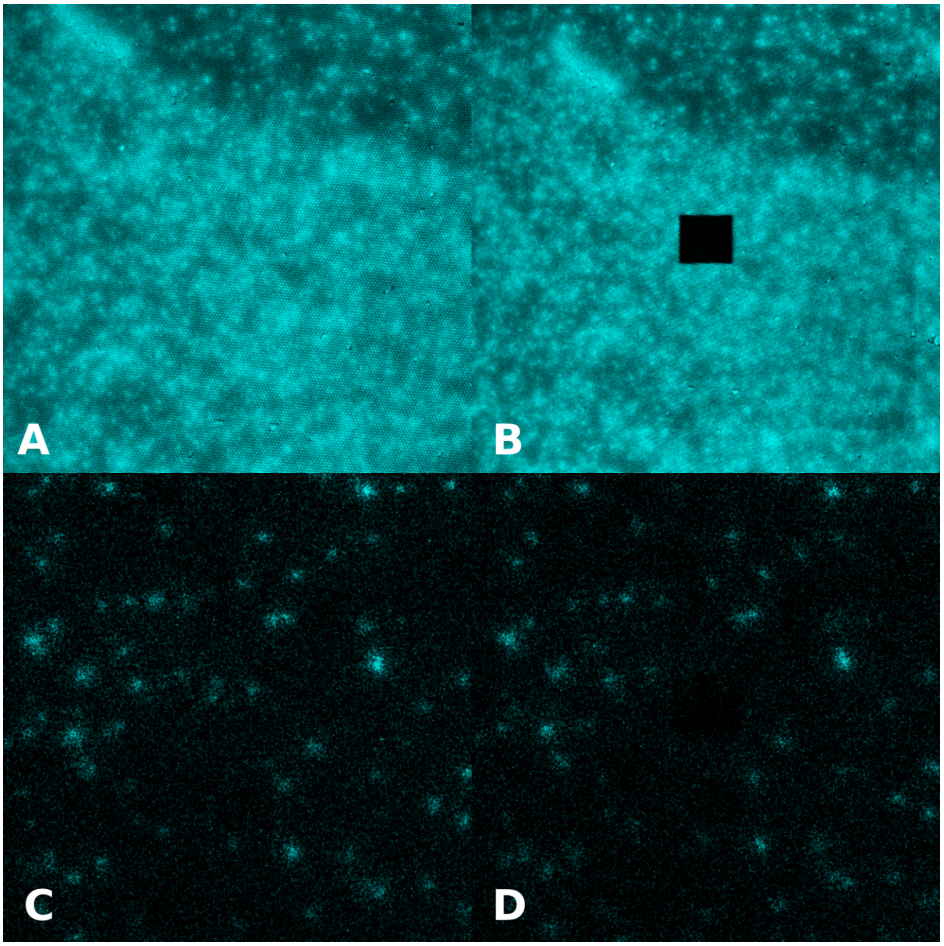

Figure 14: *The fluorescent signal seen after TSA amplification of a sample of 100ng/mL IL-1β on 2um tall SU-8 nanopillars. A) shows the fluorescent signal after TSA amplification. B) shows A after bleaching a central square. C) shows the fluorescent signal after TSA amplification when no IL-1β standard was added. D) shows C after bleaching a central square.*

A strong fluorescent signal was seen after TSA amplification of a sample treated with a 100ng/mL concentration of IL-1β (figure 14A). A clear dark square was seen after bleaching a section of this sample, as seen in figure 14B. Small amounts of signal were visible when no IL-1β standard was added to the sample, as seen in figure 14C. Bleaching was also observed in this signal, as seen in figure 14D. This indicated that there was some nonspecific binding between the CF640R and APTES/capture antibody coating in this sample. The nonspecific binding of CF640R on APTES/capture antibody coated glass and 2um SU-8 nanopillars after TSA amplification was compared, as shown in figure 15.

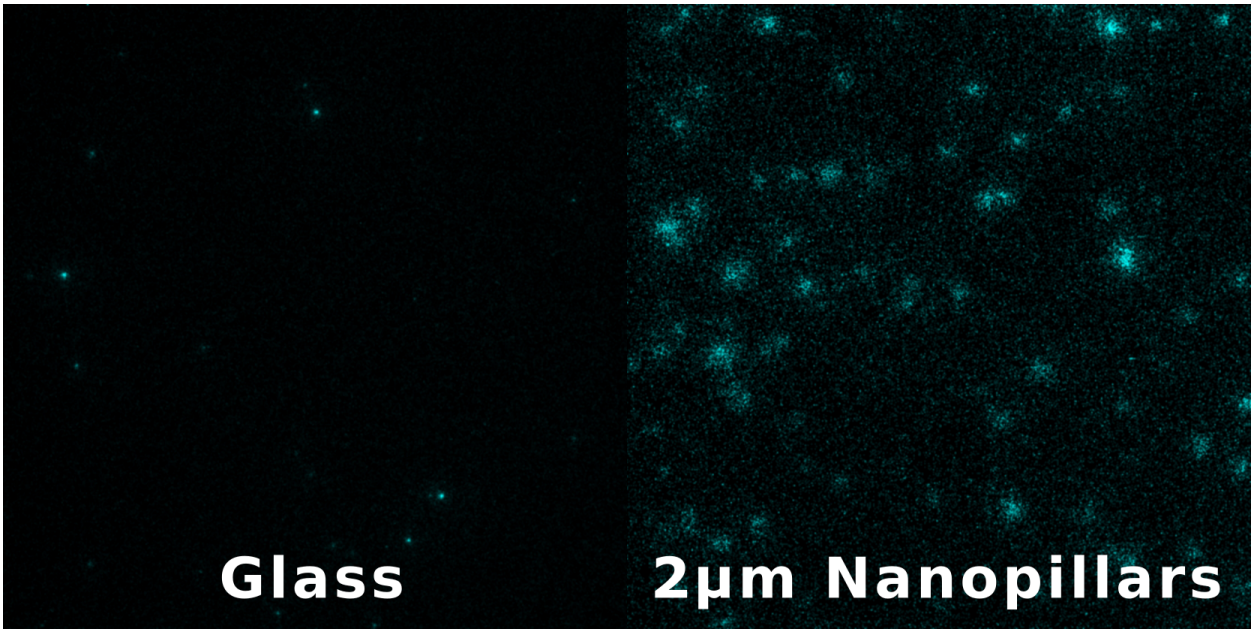

Figure 15: *The fluorescent signals due to nonspecific binding of CF640R on APTES/capture antibody coated glass and 2µm tall nanopillars after TSA amplification.*

The nonspecific binding was higher after TSA amplification for the 2µm SU-8 nanopillar sample, which was likely due to either the increased surface area the nanopillars presented for potential binding of CF640R, or the different surface and cleaning procedure used for SU-8 compared to glass.

To try to reduce nonspecific binding between the CF640R streptavidin and APTES/capture antibody surface, a premade conjugate of CF640R streptavidin/detection antibody was tested. The conjugate molecule would also be the simplest IL-1β detection method when attempting live-cell imaging, as it can be added directly into the cell medium during imaging, making it important to establish its properties prior to cell work. Again, the higher concentration of 100ng/mL IL-1β was added to each sample. The results of this assay on 2um plasma cleaned SU-8 nanopillars can be seen in figure 16.

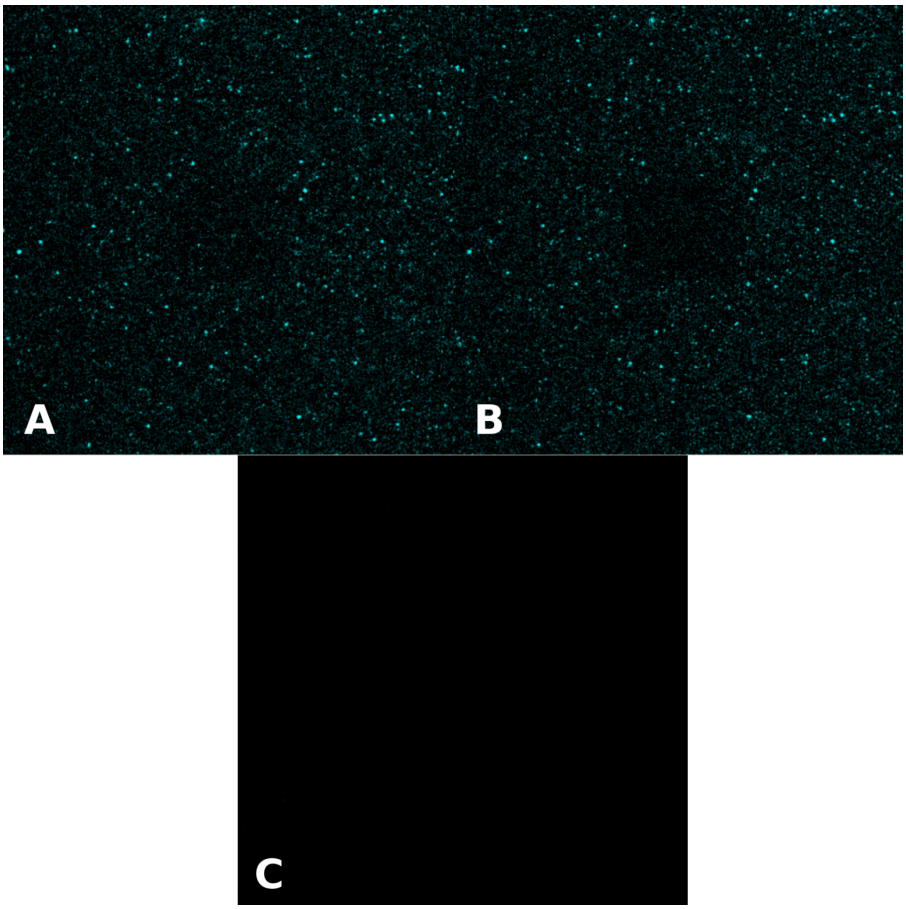

Figure 16*: The fluorescent signal from an assay run with CF640R streptavidin/detection antibody conjugate on a 2μm SU-8 nanopillar sample. A) shows the fluorescent signal after 100ng/mL IL-1β was added to the sample, and CF640R streptavidin/detection antibody conjugate was added as the detection medium. B) shows A after bleaching a central square. C) shows a negative control where no IL-1β was added during the assay.*

While the signal from the CF640R streptavidin/detection antibody conjugate was not as strong as that from the TSA amplification, it was still visible as shown in figure 16A. The weak signal was also able to be bleached, as shown in figure 16B. The negative control where no IL-1β was added to the sample showed no fluorescent signal. This indicated that the nonspecific binding was successfully reduced when using the CF640R streptavidin/detection antibody conjugate compared to free CF640R. Additionally, the ability to see a signal at a high concentration of IL-1β standard indicated it could be possible to directly detect the secretion of IL-1β from

stimulated cells using CF640R streptavidin/detection body in the detection medium in subsequent experiments.

THP-1 stimulation

Stimulation on flat glass and on nanopillars

In order to test whether the THP-1 ASC-GFP cells would grow normally, and be able to differentiate and be stimulated to release IL-1β on a glass surface, supernatants from cells grown on different surface treatments of glass were measured for IL-1β when cells were both stimulated with LPS and nigericin, a standard method for NLRP3 inflammasome activation,[40] and unstimulated. The results of this can be seen in table 8. Cells grown on untreated glass, KOH washed glass, and APTES/capture antibody coated glass all were able to grow normally, and release IL-1β into the supernatant when stimulated. Normal adherence and cell spreading was observed via microscopy, indicating normal cell growth (data not shown).

Table 8: *The measured IL-1β concentration in the supernatant taken from THP-1 cells grown and differentiated on various surfaces and surface treatments.*

Surface	Stimulation	IL-1β concentration (ng/mL)	Standard deviation
Untreated glass	Unstimulated	0.12	0.01
	LPS and nigericin	1.82	2.35
1M KOH washed glass	Unstimulated	0.04	0.04
	LPS and nigericin	1.47	0.39
0.5%APTES + 4μg/mL coated glass	Unstimulated	0.12	0.01
	LPS and nigericin	0.95	0.07

A similar test was performed to determine whether the THP-1 ASC-GFP cells would grow normally and be able to differentiate and release IL-1β on 2um SU-8 nanopillars. Supernatants

from cells grown on glass and 2um tall nanopillars were tested for IL-1β after no stimulation and LPS + nigericin stimulation. The results of this can be seen in table 9. The concentration of IL-1β in the supernatant of unstimulated cells grown on both glass and 2um tall nanopillars was very low, 0.17±0.004ng/mL and 0.07±0.01ng/mL respectively. Stimulation by LPS and nigericin of cells grown on both glass and 2um tall nanopillars caused the release of IL-1β, shown in the measured IL-1β concentration of 2.91±0.43ng/mL for cells grown on glass and 4.10±0.44ng/mL for cells grown on 2um tall SU-8 nanopillars.

Table 9: *A comparison of the release of IL-1β into the supernatant by stimulated and unstimulated THP-1 cells grown on KOH washed glass and plasma cleaned, 2um tall nanopillars.*

Surface	Stimulation	IL-1β concentration (ng/mL)	Standard deviation
1M KOH washed glass	Unstimulated	0.17	0.004
	LPS and nigericin	2.91	0.43
Plasma cleaned 2um nanopillars	Unstimulated	0.07	0.01
	LPS and nigericin	4.10	0.44

Prior to stimulation, confocal microscopy was used to observe the morphology of the differentiated THP-1 cells on 2um tall nanopillars. As shown in figure 17, normal cell morphology was observed after PMA differentiation.

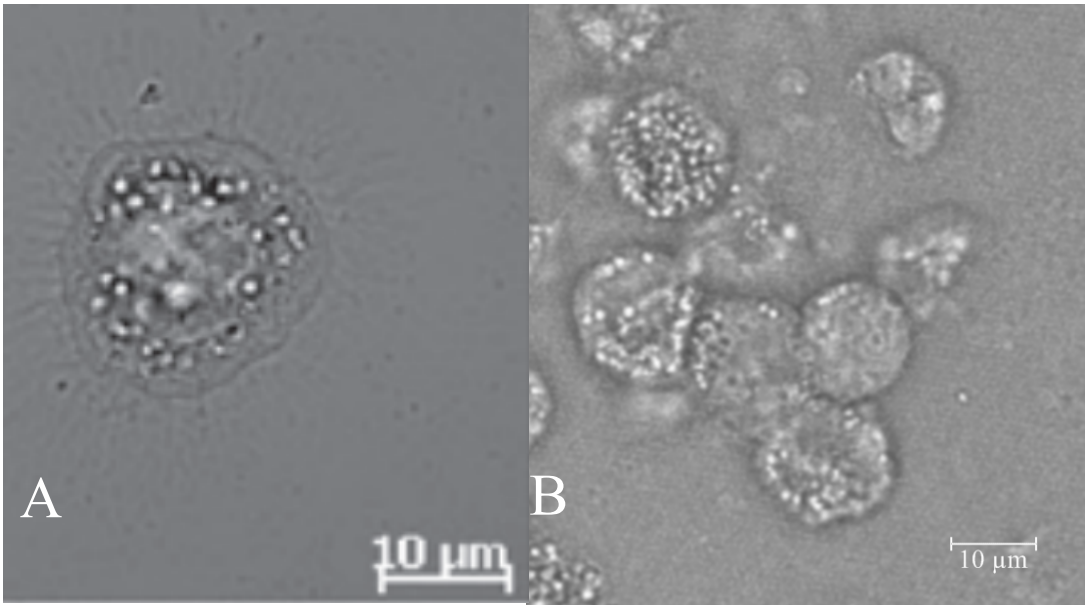

Figure 17: *A comparison of THP-1 cell morphology after PMA differentiation on polystyrene [58](A) and 2um tall plasma cleaned SU-8 nanopillars coated with APTES/capture antibody (B).*

THP-1 confocal imaging

Initial live-imaging studies are shown in figure 18. THP-1 cells were seeded at a concentration of $3.5x10^5$ cells/mL on 2um tall SU-8 nanopillars that had been coated with APTES/capture antibody and blocked with 1% BSA. The cells were stimulated to differentiate using 100ng/mL PMA, over 72 hours and allowed to rest in media without PMA for 24 hours prior to the imaging procedure. Prior to imaging, cells were stimulated with 1µg/mL LPS in RPMI for 3 hours. Subsequently the media was changed for the detection medium, containing 150ng/mL CF640R/detection antibody conjugate and 10uM nigericin. Imaging was started following the addition of the detection medium to the cells. Approximately 45 minutes after the addition of nigericin, ASC spot formation could be seen in a number of cells. Little to no fluorescent signal was observed relating to the fluorescence of CF640R, however.

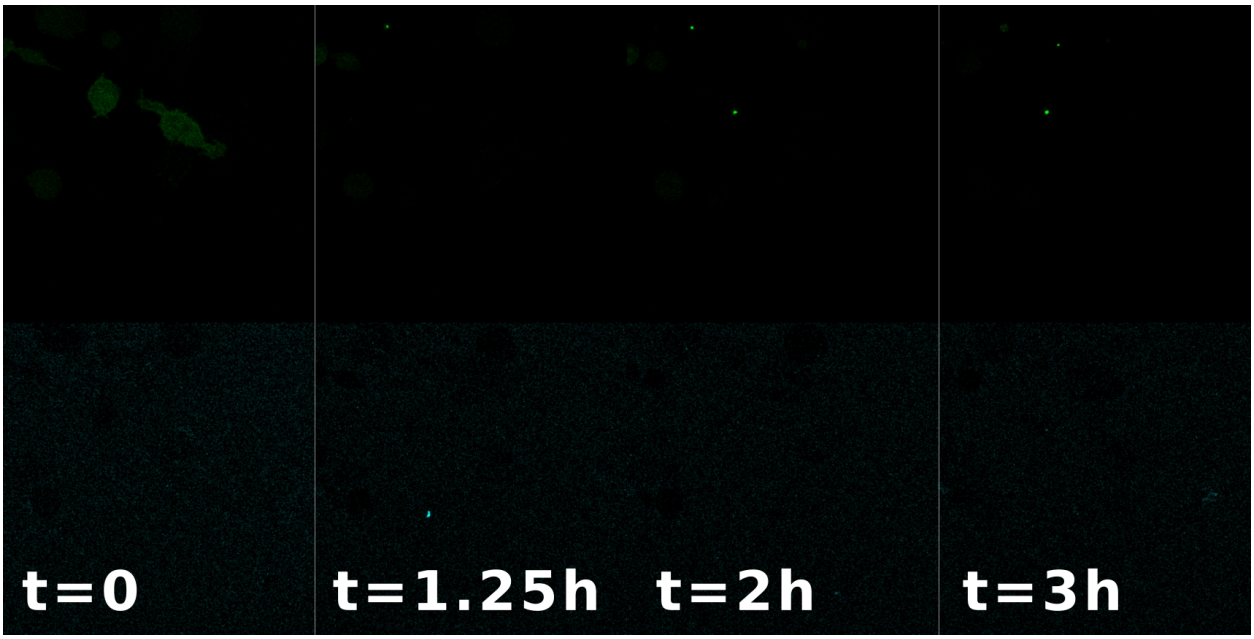

Figure 18: *Live THP-1 imaging after stimulation with LPS and Nigericin. The top image shows the GFP channel, while the bottom image shows the fluorescence due to CF640R streptavidin for each time point. Images were taken starting when nigericin was added at t=0, through t=3 hours.*

Initially, the entire cell showed fluorescence in the GFP channel, as shown in the t=0 time point in figure 18. After two hours of stimulation, ASC specks can be seen in the GFP channel, however no fluorescent signal due to bound CF640R is seen. At three hours, ASC specks can still be seen, however there is still no visible fluorescent signal due to CF640R bound to the nanopillar surface. The weak fluorescent signal seen due to CF640R is likely due to the presence of CF640R in the media. This can be seen by the dark circles outlining cells at the t=0 timepoint. The presence of these dark circles indicates that to focal plane of the microscope was too high, as fluorescence due to CF640R binding to secreted IL-1β would be expected to be seen directly underneath cells. The exclusion of the detection medium in the focal plane indicates that the cell was partially in focus, and the area underneath the cell was not. The high focal plane was likely due to focus drift in the microscope over the period of the time-lapse, as the autofocus system on the microscope being used was defective.

Instead of attempting live imaging, imaging was also performed after stimulating the cells with LPS and nigericin and subsequently fixing the cells using PFA. Results of PFA fixation after LPS and nigericin stimulation, and PFA quenching are shown in figure 19. For both the quenched and unquenched PFA fixed samples, CF640R signal was seen bound to the surface of the cell and no significant signal was seen bound to the nanopillar surface.

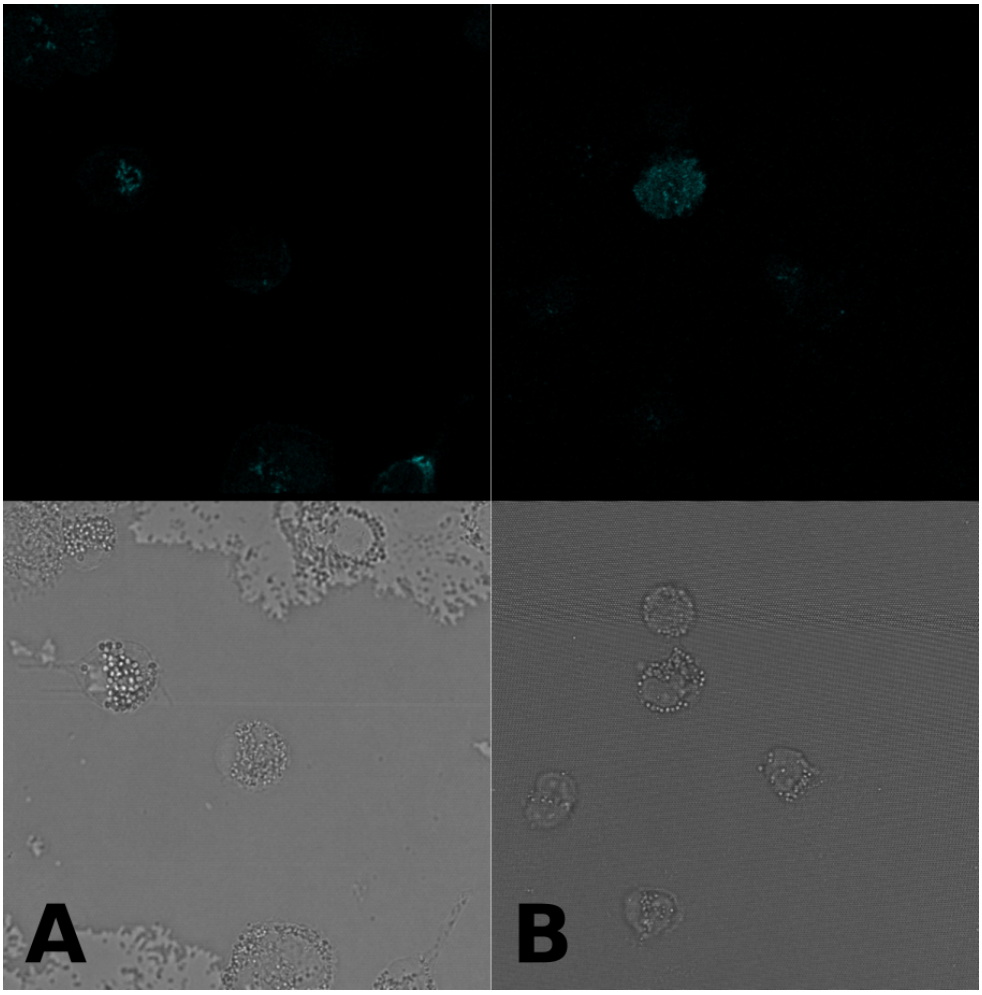

Figure 19: *Fluorescent signal and microscopy of cells after LPS and nigericin stimulation and PFA fixation. The top image shows the fluorescence due to bound CF640R. A) shows a 4% PFA fixation. B) shows a 4% PFA fixation which was quenched with 100mM glycine and 100mM NH_4Cl after fixation and before adding detection antibody and CF640R.*

It is apparent from figure 19 that the quenching procedure used was not adequate, as the observed fluorescent signal is likely caused by CF640R streptavidin binding to PFA with

residual activity. Therefore, PFA fixation was not determined to be a viable method for this type of imaging.

To avoid focal drift due to the defective microscope autofocus system during a time-lapse, imaging after 1 hour of nigericin, without PFA fixation and using CF640R/detection antibody conjugate was also performed. The results of this imaging can be seen in figure 20. In figure 20A, ASC specks are visible in stimulated cells. In figure 20B, the dark outlines of cells can be seen in the fluorescent signal of the media. This indicates that the surface where IL-1β capture should have occurred was not in focus. Additionally, some brighter larger areas, and brighter small spots can be seen. These spots could have been due to cell debris binding the CF640R/detection antibody conjugate.

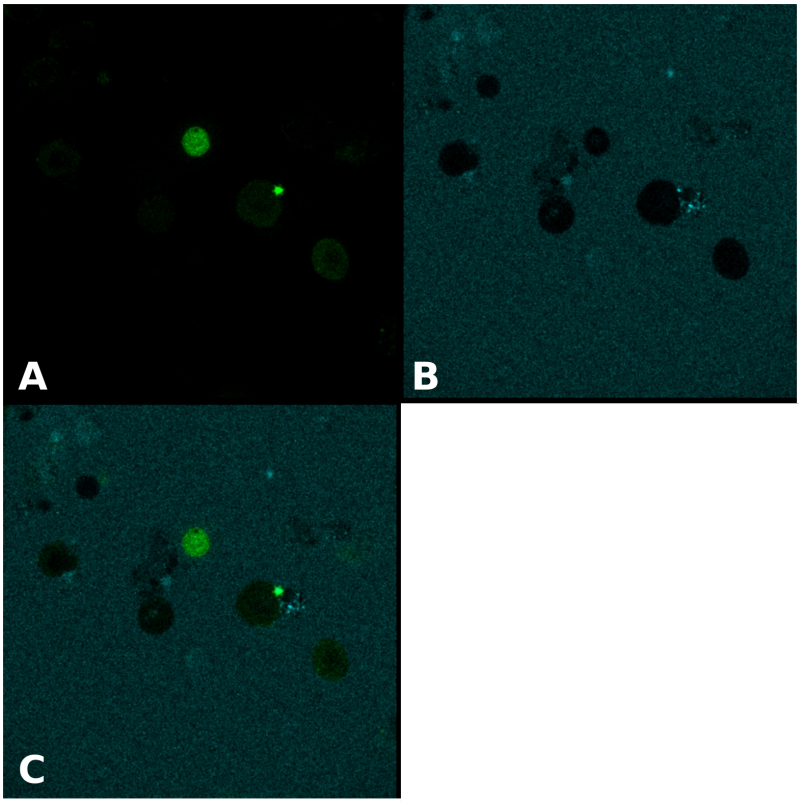

Figure 20: *Images taken of live cells stained with CF640R/detection antibody after one hour nigericin stimulation. A) shows the GFP fluorescence and ASC specks that have formed on some cells. C) shows the fluorescent signal from the CF640R/detection antibody conjugate in the media, as well as some brighter areas around cells. C) shows an overlay of A and B.*

Some brighter areas can also be seen, although these could be due to auto-fluorescence of the cells. As can be seen in figure 20C, the overlay of GFP and brighter areas of fluorescent signal from CF640R are not always near each other.

In order to confirm that IL-1β was being released by the LPS+nigericin stimulated THP-1 cells and could be detected fluorescently, TSA amplification was performed after stimulation of the cells. The TSA procedure was performed on THP-1 cells grown on 2um SU-8 nanopillars, coated in APTES/capture antibody and blocked with 1% BSA. TSA amplification was started 2 hours after 10uM nigericin was added to the cells, to enable enough time for significant IL-1β release from the cells, and binding of the IL-1β to the capture antibody This process washed the cells off, but as shown in figure 21, revealed a strong fluorescent signal due to bound IL-1β on the SU-8 nanopillar surface.

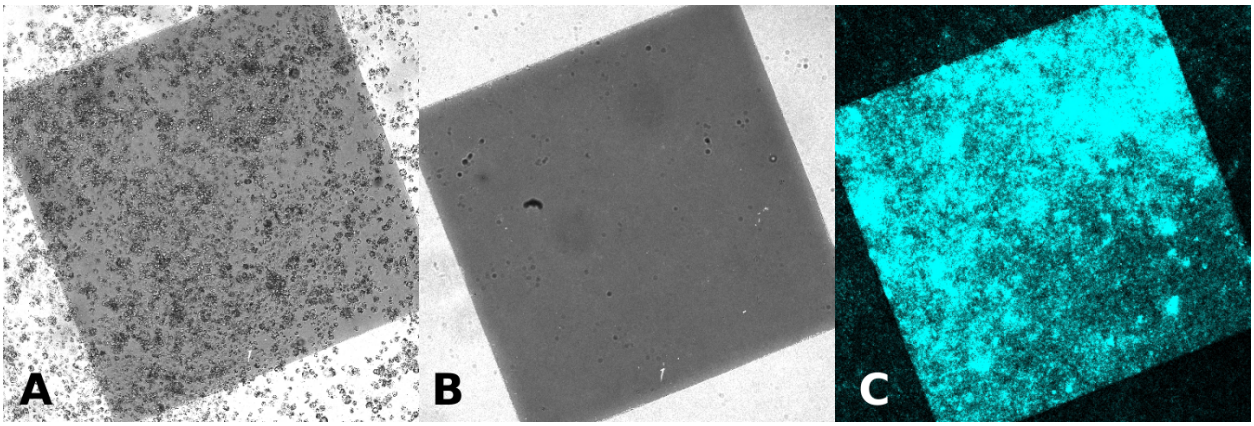

Figure 21: *The results of imaging (using a 10x air objective) TSA amplification after THP-1 stimulation with LPS and nigericin. A) shows the nanopillar coated area in gray, with THP-1 cells prior to stimulation with LPS and nigericin. B) shows the nanopillar area after washing the cells off using 0.05%Tween-20. C) shows the fluorescent signal after TSA amplification, indicating IL-1β was captured on the nanopillar surface.*

This result indicated that the fluorescent signal due to bound IL-1β without TSA amplification may have been too weak to be seen over background fluorescence, or cell autofluorescent signals. Interestingly, the fluorescent signal is much stronger on the SU-8 nanopillars than on the

flat glass surface, the surface geometry could be strongly increasing the fluorescent signal due to a larger surface area being available for bound IL-1β and TSA amplification.

DISCUSSION

Glass surface ELISA

APTES was used to immobilize antibodies onto a glass surface through covalent bonding, and this surface coating was capable of detecting IL-1β in solution with low amounts of nonspecific binding. This type of chemistry has commonly been shown to be able to immobilize proteins to Si-OH groups on oxidized surfaces.[28] DMP was also shown to be able to immobilize the capture antibody to a similar degree of effectiveness as APTES. The sample preparation procedure was much longer for DMP than APTES, however, making APTES a better candidate for the development of a simple, efficient assay.

SU-8 and nanopillar ELISA

Different types of surface treatments of glass and SU-8 were tested in order to determine the best treatment for maximum IL-1β capture using APTES, and minimal nonspecific binding of detection antibody and streptavidin-HRP during the assay. While the absorption measured on plasma treated SU-8 was less than the absorption measured on KOH treated glass, there was concern for nanopillar stability after treatment with KOH, making plasma cleaning a more viable option for surface treatment of SU-8. Plasma cleaned samples of SU-8 did show sufficient absorption levels in the HRP ELISA, and had already been shown to be compatible with nanopillars of varying dimensions.[16] Making this the preferred surface treatment for SU-8 going forward.

Imaging of fluorescent detection system

ATTO 647N-streptavidin

Two fluorescent molecules were tested for their effectiveness for fluorescently labeling the detection antibody bound to captured IL-1β. When testing the optimal concentration of ATTO 647N-streptavidin, the gain needed to be turned up significantly, and frame accumulation was required to attempt to visualize the fluorescent signal on a KOH treated glass surface. When testing different concentrations of IL-1β with this detection method, no clear pattern of increasing fluorescent signal as concentration of added IL-1β was increased could be seen. The cause of this was expected to be due to hydrophobicity of the ATTO 647N streptavidin molecule, causing it to bind nonspecifically to the coated glass surface.[44] Due to this, a less hydrophobic molecule, CF640R streptavidin conjugate, was used in subsequent experiments.[44]

CF640R-streptavidin

Nonspecific binding of the CF640R molecule was determined to be very low on APTES/capture antibody-coated KOH glass surface, consistent with the low hydrophobicity of this molecule.[44] Only very weak signals were visible when attempting to detect 1ng/mL IL-1β, indicating this may be too low of a concentration of IL-1β to be detected using fluorescent labeling. Other studies used IL-1β concentrations of 100ng/mL for the testing of their fluorescent detection system, and this higher concentration was also estimated to be present in close proximity to cells releasing IL-1β, indicating this may be a more realistic concentration to test.[10]

TSA Amplification

TSA amplification was used as a strategy to increase the sensitivity of the assay. Concentrations of IL-1β as low as 0.25 ng/mL were able to be detected using this system. This was significantly higher assay resolution than seen in other studies, which used concentrations of 100ng/mL IL-1β

in their fluorescent detection systems.[10] The ability to detect lower concentrations of IL-1β was due to TSA amplification enabling the binding of multiple fluorescent molecules to one detection antibody, allowing for brighter signals to be seen.[31] A strong fluorescent signal was also visible when performing TSA amplification on SU-8 nanopillars. This indicated it was possible to visualize the fluorescent signal from captured IL-1β on SU-8 nanopillars.

CF640R/detection antibody conjugate

To minimize nonspecific binding and test the most simple detection media for live-cell imaging, a conjugate of CF640R/detection antibody was tested using a concentration of 100ng/mL IL-1β. Although weak, the visible signal indicated that the system should be able to image concentrations down to 100ng/mL IL-1β during live-cell imaging. However, the weak fluorescent signal indicated that high laser powers may need to be used when moving to live cell imaging, potentially harming the cells.[59]

THP-1 confocal imaging

Live cell time-lapse

Live cell time-lapses were performed to attempt to simultaneously image the cells and detect the secretion of IL-1β from stimulated THP-1 ASC-GFP cells. When nigericin and the detection media had just been added at the start of the imaging, green fluorescence was seen throughout the cells. Additionally, dark circles where the cells were could be seen in the channel imaging fluorescence from CF640R, indicating that the media was slightly fluorescent due to the free CF640R/detection antibody conjugate, and the cells had not taken up any of the detection media. Pyroptosis and loss of membrane integrity was observed in the morphology of the cells after 1.25 hours of imaging, consistent with previous studies showing pyroptosis in cells after treatment with LPS and nigericin.[40] After 3 hours of imaging, IL-1β should have been released from the

cells into the media at high concentrations in the direct vicinity of stimulated cells, and should have been bound by the capture antibody that was immobilized on the surface of the nanopillars.[23, 40] This bound IL-1β should then have bound with the detection antibody/CF640R streptavidin conjugate in the media, to create a visible fluorescent signal underneath the stimulated cells. No fluorescent signal was visible, however. This could have been to focal drift due to the malfunctioning autofocus of the microscope, or due an inability to measure a weak fluorescent signal using this method.

The use of a detection antibody/CF640R streptavidin conjugate remains the most promising for the study of IL-1β secretion kinetics, however the weak signal seen when testing this with 100ng/mL IL-1β needs to be overcome.

PFA cell fixation

To enable imaging after stimulation of the cells had occurred, PFA cell fixation was performed. PFA fixation resulted in PFA binding the CF640R molecule to the cell surface. This was likely due to the fact that PFA can bind the amine groups of the detection antibody, causing the surface of the cell itself to be coated in the detection antibody.[60] To avoid this, the PFA was quenched using the quenching procedure, however this procedure was also not able to prevent CF640R from binding to the treated cells instead of the surface beneath, suggesting that cell fixation using PFA was not a viable alternative to live-cell imaging.

Imaging after nigericin stimulation

Another strategy to avoid the problem of focus drift during long time lapses was to image the cells after one hour of nigericin stimulation and to manually locate fluorescent areas. Some fluorescence was seen, however it was not localized to the nanopillar surface. Cell autofluorescence is a known phenomenon, however, so this detected signal could have been due

to autofluorescence of the THP-1 cells themselves.[61] To determine if IL-1β was successfully being captured on the nanopillar surface following THP-1 stimulation, TSA amplification was performed on the nanopillar surface after the cells had been stimulated. This washed the cells off of the surface, eliminating any fluorescent signals due to cell autofluorescence. A strong fluorescent signal was seen following TSA amplification.

TSA amplification, however, is not a method that is compatible with live-cell imaging, as it requires multiple wash steps which damage and detach the cells from the surface. Additionally, there may be challenges with the resolution of TSA amplification. High cell density was used in the experiment to maximize IL-1β secretion events, however, this could have caused signals to overlap during the TSA amplification procedure. Optimization of cell seeding density on the nanopillars will be required in order to determine whether single-cell resolution is possible with TSA amplification. Additionally, saturation during TSA amplification could cause the sensitivity of this type of assay to be low. Reducing incubation time with the TSA substrate could reduce saturation during this procedure.

A benefit of the use of TSA amplification meant that high laser powers were not needed for signal detection. Additionally, this method of detecting IL-1β secretion using can be done using confocal or wide field microscopy, while previous studies used more specialized TIRF microscopy for IL-1β detection.[10]

CONCLUSIONS

In this project, it was shown that SU-8 nanopillars can be functionalized using a one-step coating procedure of the capture antibody mixed with APTES. This type of surface coating was shown to provide strong signals using a standard HRP/TMB ELISA system, and also showed low amounts of nonspecific binding in these assays.

When shifting the system to use fluorescent-labeled streptavidin molecules, nonspecific binding due to the interaction of ATTO 647N was reduced by using a fluorophore that was less hydrophobic, CF640R. When testing the system with CF640R, signals from 1ng/mL IL-1β were very weak, and difficult to distinguish from background noise. Signals from 100ng/mL IL-1β were able to be visualized, however. TSA signal amplification was successfully implemented in samples incubated with 1ng/mL IL-1β and 100ng/mL IL-1β, resulting in a strong fluorescent signal from these samples, indicating that IL-1β was captured on the nanopillar surfaces. Non-specific binding was shown to be minimal during TSA amplification as well. Once the fluorescent detection system was developed, cell studies were performed.

THP-1 ASC GFP cells grew and differentiated normally on the coated nanopillar system. Additionally, they were observed to release IL-1β when stimulated with LPS and nigericin while grown on the nanopillars. While fluorescent cytokine detection with simultaneous live-cell imaging was not successfully performed during this experiment, promising results in the development of this method were achieved. Importantly, normal THP-1 ASC GFP behavior on the coated surface, as well as the ability to detect cytokine concentrations of 100ng/mL using TSA amplification, or by using the CF640R/detection antibody conjugate that was created, show that further optimization of the system could lead to the successful combination of cytokine detection and high-resolution cell imaging on a single cell level. TSA amplification was also

shown to be able to detect IL-1β concentrations down to 0.25ng/mL. Additionally, it was successfully demonstrated that IL-1β secreted from THP-1 cells stimulated with LPS and nigericin was captured on SU-8 nanopillars and was visualized using TSA amplification following cell stimulation.

FUTURE DIRECTIONS

In order to fully achieve the goal of combining cytokine detection with high resolution cell imaging on a single cell level, optimization of the system described in this project must be continued. Several experiments have been identified that may help with further development of this project.

As the fluorescent signal was observed to be quite weak unless TSA amplification was used, different surface chemistries could be used to attempt to achieve a higher density of capture antibody bound to the nanopillar surface. This would enable a brighter fluorescent signal to be seen when trying to detect cytokine release. For example, the DMP surface coating that had been tested using the HRP/TMB ELISA system could be tested in the fluorescent system. Different surface treatments could be performed on the SU-8 prior to coating with APTES/capture antibody, and different concentrations of APTES and capture antibody could be tested to try to optimize fluorescent signal strength in the assay.

As it was shown that IL-1β was captured following THP-1 stimulation, different detection media should be tested to try and increase the fluorescent signal from bound IL-1β without the need for TSA amplification. A higher concentration of detection antibody could be used in the detection medium, or a different conjugation procedure could be attempted to try to load more CF640 onto the detection antibodies. This would allow for live-imaging of the secretion of IL-1β to be performed.

Once IL-1β detection and live-cell imaging is achieved, the system can be adapted to measure different cytokines. Additionally, the system could be adapted by immobilizing multiple capture antibodies on the nanopillar surface, to allow for the simultaneous measurement of different cytokine release from cells while at the same time imaging them. This type of assay has been developed using microarrays of different capture antibody spots, however mixes of antibodies have not been tested to create a heterogeneous capture antibody coating on a surface.[62] This type of the simultaneous detection of multiple cytokines would be advantageous to help study the complexity of protein networks and cytokine secretion during immune responses.[63] Steric hindrance and cross-reactivity between the targeted cytokines and capture antibodies would have to be carefully considered for the successful development of such an assay.[64]

Once optimally developed, the system will enable the study of single or multiple cytokine release with simultaneous high-resolution imaging of the cells secreting the cytokines.

Acknowledgments

I would like to thank Kai S. Beckwith for all of his help and support in the development and execution of this project, and for supervising me during the last two semesters. I would also like to thank Prof. Pawel Sikorsky for introducing me to Kai, and for his collaboration in planning this project. Thank you to Jakob Vinje, for creating all of the nanopillar samples used throughout this project. Thanks to Prof. Berit Strand for serving as the internal supervisor within the Department of Biotechnology. Thank you to everyone at CEMIR, for being welcoming and providing a great lab atmosphere. Finally, thank you to my family and friends for their support and help during the last two years.

REFERENCES

1. Rothenberg, Ellen V. "Cell lineage regulators in B and T cell development." *Nature immunology* 8.5 (2007): 441.
2. Ma, Chao, et al. "A clinical microchip for evaluation of single immune cells reveals high functional heterogeneity in phenotypically similar T cells." *Nature medicine* 17.6 (2011): 738.
3. Marcus, Joshua S., W. French Anderson, and Stephen R. Quake. "Microfluidic single-cell mRNA isolation and analysis." *Analytical chemistry* 78.9 (2006): 3084-3089.
4. Murphy, Ken, and Casey Weaver. *Janeway's immunobiology*. Garland Science, 2016.
5. Jung, Thomas, et al. "Detection of intracellular cytokines by flow cytometry." *Journal of immunological methods* 159.1-2 (1993): 197-207.
6. Lewis, Claire E. "Detecting cytokine production at the single-cell level." *Cytokine* 3.3 (1991): 184-188.
7. Czerkinsky, Cecil C., et al. "A solid-phase enzyme-linked immunospot (ELISPOT) assay for enumeration of specific antibody-secreting cells." *Journal of immunological methods* 65.1-2 (1983): 109-121.
8. Prabhakar, Uma, and Marian Kelley, eds. *Validation of cell-based assays in the GLP setting: A practical guide*. John Wiley & Sons, 2008.
9. Gazagne, Agnès, et al. "A Fluorospot assay to detect single T lymphocytes simultaneously producing multiple cytokines." *Journal of immunological methods* 283.1-2 (2003): 91-98.
10. Shirasaki, Yoshitaka, et al. "Real-time single-cell imaging of protein secretion." *Scientific reports* 4 (2014): 4736.

11. An, Xingyue, et al. "Single-cell profiling of dynamic cytokine secretion and the phenotype of immune cells." *PloS one* 12.8 (2017): e0181904.
12. Stevens, Molly M., and Julian H. George. "Exploring and engineering the cell surface interface." *Science* 310.5751 (2005): 1135-1138.
13. Salata, Oleg V. "Applications of nanoparticles in biology and medicine." *Journal of nanobiotechnology* 2.1 (2004): 3.
14. Bonde, Sara, et al. "Exploring arrays of vertical one-dimensional nanostructures for cellular investigations." *Nanotechnology* 25.36 (2014): 362001.
15. López-Romero, D., et al. "High aspect-ratio SU-8 resist nano-pillar lattice by e-beam direct writing and its application for liquid trapping." *Microelectronic Engineering* 87.4 (2010): 663-667.
16. Beckwith, Kai Sandvold, et al. "Tunable high aspect ratio polymer nanostructures for cell interfaces." *Nanoscale* 7.18 (2015): 8438-8450.
17. Lorenz, Hubert, et al. "SU-8: a low-cost negative resist for MEMS." *Journal of Micromechanics and Microengineering* 7.3 (1997): 121.
18. Walther, Ferdinand, et al. "Stability of the hydrophilic behavior of oxygen plasma activated SU-8." *Journal of Micromechanics and Microengineering* 17.3 (2007): 524.
19. Vernekar, Varadraj N., et al. "SU-8 2000 rendered cytocompatible for neuronal bioMEMS applications." *Journal of Biomedical Materials Research Part A* 89.1 (2009): 138-151.
20. Huebsch, Nathaniel, et al. "Harnessing traction-mediated manipulation of the cell/matrix interface to control stem-cell fate." *Nature materials* 9.6 (2010): 518.

21. Buch-Månson, Nina, et al. "Mapping cell behavior across a wide range of vertical silicon nanocolumn densities." *Nanoscale* 9.17 (2017): 5517-5527.

22. Kindt, Thomas J., et al. *Kuby immunology*. Macmillan, 2007.

23. Bos, E. S., et al. "3, 3′, 5, 5′-Tetramethylbenzidine as an Ames test negative chromogen for horse-radish peroxidase in enzyme-immunoassay." *Journal of Immunoassay and Immunochemistry*2.3-4 (1981): 187-204.

24. Rusmini, Federica, Zhiyuan Zhong, and Jan Feijen. "Protein immobilization strategies for protein biochips." *Biomacromolecules* 8.6 (2007): 1775-1789.

25. Kim, Dohyun, and Amy E. Herr. "Protein immobilization techniques for microfluidic assays." *Biomicrofluidics* 7.4 (2013): 041501

26. Nakanishi, Kazuhiro, et al. "Recent advances in controlled immobilization of proteins onto the surface of the solid substrate and its possible application to proteomics." *Current Proteomics*5.3 (2008): 161-175.

27. Hermanson, Greg T. *Bioconjugate techniques*. Academic press, 2013.

28. Vansant, Etienne F., Pascal Van Der Voort, and Karl C. Vrancken. *Characterization and chemical modification of the silica surface*. Vol. 93. Elsevier, 1995.

29. White, L. D., and C. P. Tripp. "Reaction of (3-aminopropyl) dimethylethoxysilane with amine catalysts on silica surfaces." *Journal of Colloid and Interface Science* 232.2 (2000): 400-407.

30. Vashist, Sandeep Kumar, et al. "Immobilization of antibodies and enzymes on 3-aminopropyltriethoxysilane-functionalized bioanalytical platforms for biosensors and diagnostics." *Chemical reviews* 114.21 (2014): 11083-11130.

31. Bobrow, Mark N., et al. "Catalyzed reporter deposition, a novel method of signal amplification application to immunoassays." *Journal of immunological methods* 125.1-2 (1989): 279-285.

32. Bobrow, M. N., et al. "The use of catalyzed reporter deposition as a means of signal amplification in a variety of formats." *Journal of immunological methods* 150.1-2 (1992): 145-149.

33. Gijlswijk, Rob PM van, et al. "Fluorochrome-labeled tyramides: use in immunocytochemistry and fluorescence in situ hybridization." *Journal of Histochemistry & Cytochemistry* 45.3 (1997): 375-382.

34. Wang, Guoji, et al. "Tyramide signal amplification method in multiple-label immunofluorescence confocal microscopy." *Methods* 18.4 (1999): 459-464.

35. McLoughlin, Eavan. *"*Protein Kinase LKB1 regulates MRP2/ABCC11 and Bile Excretion in vivo. A translational study linking Neonatal Jaundice & Adult onset Hepatocellular carcinoma*." Diss. Trinity College Dublin* (2016).

36. Garlanda, Cecilia, Charles A. Dinarello, and Alberto Mantovani. "The interleukin-1 family: back to the future." *Immunity* 39.6 (2013): 1003-1018.

37. Martinon, Fabio, Kimberly Burns, and Jürg Tschopp. "The inflammasome: a molecular platform triggering activation of inflammatory caspases and processing of proIL-β." *Molecular cell* 10.2 (2002): 417-426.

38. Shi, Jianjin, et al. "Cleavage of GSDMD by inflammatory caspases determines pyroptotic cell death." *Nature* 526.7575 (2015): 660.

39. Liu, Xing, et al. "Inflammasome-activated gasdermin D causes pyroptosis by forming membrane pores." *Nature* 535.7610 (2016): 153.

40. Gaidt, Moritz M., et al. "Human monocytes engage an alternative inflammasome pathway." *Immunity* 44.4 (2016): 833-846.

41. Van Oostrum, Jan, et al. "The structure of murine interleukin-1 β at 2.8 Å resolution." *Journal of structural biology* 107.2 (1991): 189-195.

42. Sborgi, Lorenzo, et al. "GSDMD membrane pore formation constitutes the mechanism of pyroptotic cell death." *The EMBO journal* 35.16 (2016): 1766-1778.

43. Evavold, Charles L., et al. "The pore-forming protein gasdermin D regulates interleukin-1 secretion from living macrophages." *Immunity* (2017).

44. Zanetti-Domingues, Laura C., et al. "Hydrophobic fluorescent probes introduce artifacts into single molecule tracking experiments due to non-specific binding." *PloS one* 8.9 (2013): e74200.

45. Chandler, Douglas E., and Robert W. Roberson. *Bioimaging: Current Concepts In Light & Electron Microscopy*. Jones & Bartlett Publishers, 2009.

46. Arden-Jacob, Jutta, et al. "New fluorescent markers for the red region." *Spectrochimica Acta Part A: Molecular and Biomolecular Spectroscopy*57.11 (2001): 2271-2283.

47. Westphal, Volker, et al. "Video-rate far-field optical nanoscopy dissects synaptic vesicle movement." *Science* 320.5873 (2008): 246-249.

48. Kolmakov, Kirill, et al. "Red-emitting rhodamine dyes for fluorescence microscopy and nanoscopy." *Chemistry-A European Journal* 16.1 (2010): 158-166.

49. Masters, Barry R. "Handbook of biological confocal microscopy." *Journal of biomedical optics* 13.2 (2008): 029902.

50. Paul Peter, Urone, et al. *College physics*. OpenStax College, Rice University, 2016.

51. Lewis, C.E., McGee, J.O'D. (1992) The Macrophage. IRL Press, Oxford, UK.

52. Tsuchiya, Shigeru, et al. "Establishment and characterization of a human acute monocytic leukemia cell line (THP-1)." *International journal of cancer* 26.2 (1980): 171-176.

53. Tsuchiya, Shigeru, et al. "Induction of maturation in cultured human monocytic leukemia cells by a phorbol diester." *Cancer research* 42.4 (1982): 1530-1536.

54. Schwende, Heike, et al. "Differences in the state of differentiation of THP-1 cells induced by phorbol ester and 1, 25-dihydroxyvitamin D3." *Journal of leukocyte biology* 59.4 (1996): 555-561.

55. Nishizuka, Yasutomi. "Intracellular signaling by hydrolysis of phospholipids and activation of protein kinase C." *Science* 258.5082 (1992): 607-614.

56. Vashist, Sandeep Kumar, et al. "One-step antibody immobilization-based rapid and highly-sensitive sandwich ELISA procedure for potential in vitro diagnostics." *Scientific reports* 4 (2014): 4407.

57. Fernandes-Alnemri, T., et al. "The pyroptosome: a supramolecular assembly of ASC dimers mediating inflammatory cell death via caspase-1 activation." *Cell death and differentiation* 14.9 (2007): 1590.

58. Daigneault, Marc, et al. "The identification of markers of macrophage differentiation in PMA-stimulated THP-1 cells and monocyte-derived macrophages." *PloS one* 5.1 (2010): e8668.

59. Butterfield, D. Allan, et al. "Catalytic biofunctional membranes containing site-specifically immobilized enzyme arrays: a review." *Journal of Membrane Science* 181.1 (2001): 29-37.

60. Stadler, Charlotte, et al. "A single fixation protocol for proteome-wide immunofluorescence localization studies." *Journal of proteomics* 73.6 (2010): 1067-1078.

61. Alberti, Saverio, David R. Parks, and Leonard A. Herzenberg. "A single laser method for subtraction of cell autofluorescence in flow cytometry." *Cytometry Part A* 8.2 (1987): 114-119.

62. Huang, Ruo-Pan, et al. "Simultaneous detection of multiple cytokines from conditioned media and patient's sera by an antibody-based protein array system." *Analytical biochemistry*294.1 (2001): 55-62.

63. Kingsmore, Stephen F. "Multiplexed protein measurement: technologies and applications of protein and antibody arrays." *Nature reviews Drug discovery* 5.4 (2006): 310.

64. Li, Yiwen, and W. Monty Reichert. "Adapting cDNA microarray format to cytokine detection protein arrays." *Langmuir* 19.5 (2003): 1557-1566.